Accepted Manuscript

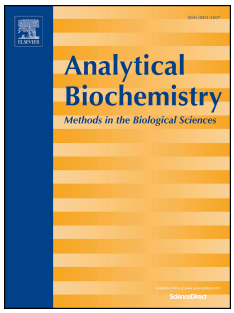

Exploring sensitivity & throughput of a parallel flow SPRi biosensor for characterization of antibody-antigen interaction

Vishal Kamat, Ashique Rafique

PII: S0003-2697(17)30077-5

DOI: 10.1016/j.ab.2017.02.007

Reference: YABIO 12627

To appear in: *Analytical Biochemistry*

Received Date: 23 November 2016

Revised Date: 6 January 2017

Accepted Date: 14 February 2017

Please cite this article as: V. Kamat, A. Rafique, Exploring sensitivity & throughput of a parallel flow SPRi biosensor for characterization of antibody-antigen interaction, *Analytical Biochemistry* (2017), doi: 10.1016/j.ab.2017.02.007.

Title: Exploring Sensitivity & Throughput of a Parallel Flow SPRi Biosensor for Characterization of Antibody-Antigen Interaction

Authors: Vishal Kamat *, Ashique Rafique
Biomolecular HTS Center, Therapeutic Proteins, Regeneron Pharmaceuticals
777 Old Saw Mill River Road, Tarrytown, NY, USA 10591

***Corresponding author**: Vishal Kamat,
Phone: +1-914-847-7771
Fax: +1-914-847-7453
Email: vishal.kamat@regeneron.com

Subject Category: Physical techniques

Highlights:

- MASS-1 produces comparable (standard deviation of 10%) kinetic binding parameters across all eight flow channels, and measured values are within 2 fold of those measured using Biacore 4000.
- MASS-1 was successfully used to perform a single injection cycle kinetics (SICK) assay which allows for high-throughput screening of biomolecular interactions.
- MASS-1 sensitivity was independent of protein immobilization level and allowed characterization of picomolar affinity antibody-antigen interactions using ultra-low density mAb surfaces.
- A high-throughput kinetic analysis of a panel of 189 monoclonal antibodies to 13 different antigens with molecular weight ranging from 14kD to 105kD produced comparable kinetic binding parameters measured to those measured on Biacore 4000.
- Collectively, the data presented in this study demonstrate that MASS-1 measures reliable binding kinetic parameters and has an appropriate combination of throughput and sensitivity to support discovery and development of therapeutic mAbs.

Keywords: Biacore, MASS-1, Surface plasmon resonance, high throughput, antibody-antigen interaction, binding kinetics

Abbreviations: real time label free (RT-LF), surface plasmon resonance (SPR), surface plasmon resonance imaging (SPRi), monoclonal antibodies (mAbs), Molecular Affinity Screening System (MASS-1), mass transport limitation (MTL), single injection cycle kinetics (SICK), multiple injection cycle kinetics (MICK), integrated fluidic cartridge (IFC), N-(3-dimethylaminopropyl)-N-ethylcarbodiimide (EDC), N-hydroxysuccinimide (NHS), fragment based drug discovery (FBDD)

ABSTRACT

Rapid growth in the field of biotherapeutics has led to an increased demand for high-throughput, label-free biosensors exhibiting high sensitivity. To support the current needs, Sierra Sensors introduced a surface plasmon resonance imaging (SPRi) based biosensor, Molecular Affinity Screening System (MASS-1). We assessed the potential utility of MASS-1 to support Regeneron's therapeutic antibody discovery. A large panel of antibody-antigen interactions was characterized using MASS-1 and the kinetic data were compared with the Biacore 4000 biosensor. Less than 10% deviation in the binding rate constants measured across eight flow channels of MASS-1 was observed. The single injection cycle kinetic assay allowed rapid measurement of binding rate constants for antibody-antigen interactions. MASS-1 sensitivity is independent of protein immobilization level and kinetic analysis performed using ultra-low density mAb surfaces allowed characterization of picomolar affinity interactions without mass transport limitation. High-throughput characterization of a panel of 189 monoclonal antibodies to 13 different antigens with molecular weights ranging from 14kD to 105kD revealed that binding kinetic parameters measured on MASS-1 were comparable to those measured on Biacore 4000. Our data demonstrate that MASS-1 measures reliable binding kinetic parameters and has an appropriate combination of throughput and sensitivity to support discovery and development of therapeutic antibodies.

1. INTRODUCTION

The global market for recombinant protein drugs is estimated to be 100 billion dollars, with therapeutic monoclonal antibodies (mAbs) constituting the largest market share (1-4). Utilization of high-throughput characterization tools during the initial screening stage is pivotal for the rapid identification of potential therapeutic mAbs. Among a wide range of biophysical, biochemical and functional characterization techniques used for biotherapeutic discovery, a real-time, label-free (RT-LF) biosensor is an important bioanalytical platform, as they enable direct measurement of the kinetics of drug binding to its target (5-10). Although currently available RT-LF platforms are sensitive enough to measure binding kinetics of small molecules to macromolecules, lack of throughput often limits their applications during the primary screening of therapeutic drugs. Parallel flow biosensors such as Biacore 4000 and ProteOn XPR36 provide the throughput to support the current mAb discovery and can screen approximately 400 mAbs per day from unpurified conditioned media (CM) as opposed to the conventional serial flow biosensors such as Biacore 3000 and Biacore T200, which can screen approximately 100 mAbs (11-13). However, both Biacore 4000 and ProteOn XPR36 lack sensitivity and designing kinetics assay with a binding response of less than 5RU is challenging. Therefore, there is a continuous demand for high-throughput biosensors with high sensitivity to support the needs of current biotherapeutic industry.

MASS-1, a relatively new biosensor platform from Sierra Sensors, is an eight-channel surface plasmon resonance imaging (SPRi) based biosensor that allows simultaneous injection of up to eight different samples into independent flow channels (Figure 1). Each flow channel contains two individually addressable detection spots; one is used as the reference spot while the other is used as the active spot. MASS-1 can thus simultaneously detect up to sixteen binding events

across the entire sensor surface. The proprietary Hydrodynamic Isolation™ (HI) technology allows uniform and simultaneous delivery of samples across all eight flow channels. The novel SPRi detection system of MASS-1 enables detection of binding events with high sensitivity (14). These device features encouraged us to evaluate the performance and sensitivity of MASS-1 for the characterization of mAb-antigen interactions.

It has been previously reported that surface charge and sensor chemistry can affect kinetic analysis of antibody-antigen interactions (15,16). We therefore evaluated the performance of MASS-1 by comparing binding rate constants measured on MASS-1 with the values measured using Biacore 4000 under diverse assay formats on a panel of mAbs binding to antigen with molecular weights ranging from 3.5kD to 105kD. The throughput capability of MASS-1 was evaluated using the single injection cycle kinetics (SICK) assay format, and the accuracy of the measured binding parameters were compared to those measured using the standard multiple injection cycle kinetics (MICK) format on Biacore 4000 and MASS-1. The effect of protein surface density on the sensitivity of MASS-1 was investigated by performing MICK assay on sensor surface immobilized with different densities of anti-human Fcγ capture mAb. The ability of MASS-1 sensitivity to characterize high affinity binding interactions was also tested by performing kinetic assays on an ultra-low density mAb surface to overcome mass transport limitation (MTL). Finally, a panel of 189 mAb-antigen interactions was characterized to assess the utility of MASS-1 to perform high throughput kinetic screening of mAbs.

Figure 1: Schematic of MASS-1 Integrated Fluidic Cartridge Design

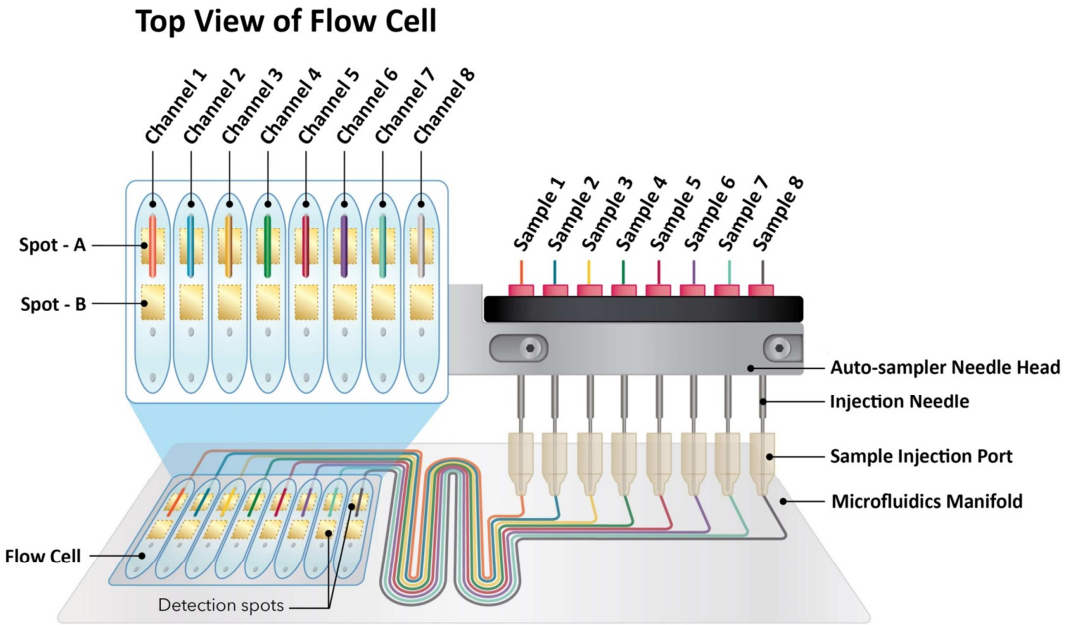

MASS-1 can simultaneously inject up to eight different samples into independent flow cells, labeled as Channel-1 through Channel-8. Each flow channel contains two individually addressable detection spots (designated as Spot-A and Spot-B), for a total of 16 binding measurements across the entire sensor surface.

2. MATERIALS & METHODS

2.1. Reagents

Coupling reagents, N-(3-dimethylaminopropyl)-N-ethylcarbodiimide (EDC) and N-hydroxysuccinimide (NHS), ethanolamine–HCl (Catalog# BR100633), anti-human Fcγ specific capture mAb (Catalog# BR-1008-39) and CM5 sensor chips (Catalog# BR-1005-30) were purchased from GE Healthcare. HCA sensor chips were purchased from Sierra Sensors (Catalog# SPR-AS-HCA). Sodium acetate, pH 5.0 was purchased from Ricca Chemical (Catalog# 61-1). All the recombinant proteins were expressed and purified in-house using stable CHO cell lines. Unless specified, all the antigens used in this study are monomeric ectodomain of the single transmembrane receptor expressed with a C-terminal 6xHis tag. Owing to the sensitive nature, we are unable to provide the identities of the antigens and all the antigens used in this study are referred based on their molecular weights. Lyophilized peptide was custom ordered from Celtek and reconstituted to 5mg/mL in Dulbecco's phosphate-buffer saline before use. HEPES (Teknova, Catalog# H1035), NaCl (Gibco, Catalog# 24740-011), EDTA (BDH, Catalog# BDH8730-1) and Tween-20® (Bio-Rad, Catalog# 161-0781) were used to prepare running buffer.

2.2. Immobilization of anti-human Fcγ mAb on MASS-1

The blank HCA sensor surface was first conditioned using alternated 30 second injections of Buffer A (1M NaCl, 10mM NaOH) and Buffer B (100mM HCl). Conditioning was performed sequentially over Spot A, Spot B, and the entire sensor surface. Immobilization of proteins was performed using 10mM sodium acetate, pH 5.0 as the running buffer at a flow rate of 12.5µL/min. The blank HCA sensor surface was first activated by injecting a 1:1 (v/v) mixture of 400mM EDC and 100mM NHS (prepared in deionized water) for 8-10 minutes followed by injection of monoclonal mouse anti-human Fcγ (10-15µg/mL) prepared in 10mM sodium acetate, pH5.0 for 8-10 minutes. Remaining active groups on the HCA sensor surface were blocked by injecting 1M ethanolamine, pH 8.5 for 8 minutes. Uncoupled residual protein was removed by treating the sensor surface with 10 seconds injections of 10mM glycine–HCl, pH1.5, 8-10 times before performing binding studies.

2.3. Binding studies performed on MASS-1

Unless specified, all of the binding studies were performed in freshly prepared, filtered and degassed running buffer containing 10mM HEPES, 150mM NaCl, 3mM EDTA and 0.05% Tween-20® (HBS-ET) at 25°C. Before performing binding studies, the anti-human Fcγ mAb immobilized HCA sensor surface was equilibrated with running buffer by priming the instrument at least three to four times. The desired level of antigen-specific mAb was captured on Spot-B, and analyte was injected for 4 or 6 minutes at a flow rate of 30µL/min. Dissociation of the bound analyte was achieved in running buffer for 10 or 15 minutes. Running buffer without analyte was injected to allow subtraction of baseline drift resulting from the natural dissociation of captured mAb from the coupled mouse anti-human Fcγ surface. At the end of each cycle, the mAb surface was regenerated by injecting 10mM glycine, pH 1.5 or 20mM phosphoric acid for 8-12 seconds.

Channel-to-channel variability in binding kinetics was investigated by capturing the same antigen-specific mAb across all eight channels and injecting serial dilutions of antigen over mAb

captured surface. The effect of protein surface density on instrument noise was studied by immobilizing different levels of anti-human Fcγ capture mAb (approximately 400RU; 1,000RU; 2,500RU and 10,000RU) across different flow channels as described above. Antigen-specific mAbs were captured at low density and varying concentrations of analyte were injected. Mass transport-limited, high affinity mAb-antigen interactions were characterized by capturing antigen-specific mAbs at different densities on HCA sensors immobilized with ~8000RU of anti-human Fcγ capture mAb followed by the injection of different serial dilutions of antigen.

2.4. Binding studies performed on Biacore 4000

A CM5 sensor was first immobilized with anti-human Fcγ mAb using a standard protocol. Briefly, the chip was activated by injecting a 1:1 (v/v) mixture of 400mM EDC and 100mM NHS at a flow rate of 10µL/min for 10 minutes. Monoclonal mouse anti-human Fcγ (10µg/mL) prepared in 10mM sodium acetate, pH5.0 was then injected at a flow rate of 10µL/min for 7-10 minutes. Finally, 1M ethanolamine was injected for 10 minutes at a flow rate of 10µL/min. During the entire immobilization procedure, 10mM sodium acetate, pH 5.0 was used as running buffer. Using this procedure, immobilization of 5000-8000 RU of anti-human Fcγ was achieved. The anti-human Fcγ immobilized surface was used to capture an antigen-specific mAb. Different concentrations of antigen (two-fold or three-fold serial dilutions) were then injected over the captured mAb surface for 4 minutes at a flow rate of 30µL/min. Dissociation of antigen was achieved in running buffer for 10 minutes. Injection of running buffer without analyte was performed to allow double reference subtraction.

2.5. SICK and MICK assays performed on MASS-1

The SICK assay was performed by capturing same antigen-specific mAb across different flow channels immobilized with approximately 10,000RU of anti-human Fcγ capture mAb. Six serial dilutions of analyte were injected simultaneously across different flow channels. A buffer injection cycle preceding analyte injection was used for double reference subtraction. The MICK assay was performed as described earlier by first capturing mAb and sequentially injecting an analyte titration series.

2.6. Comparability Study Performed Under High-Throughput Screening Mode

A comparability study was performed on Biacore 4000 and MASS-1 under high-throughput screening mode. A panel of 189 mAbs binding to 13 different antigens with molecular weights ranging from 14kDa to 105kDa was used in this study. Binding rate constants were determined by injecting five to six analyte concentrations, serially diluted by three-fold in running buffer over the anti-human Fcγ captured mAb surfaces.

2.7. Data processing and analysis

MASS-1 and Biacore 4000 binding data were processed using AnalyserR2 and Biacore 4000 evaluation software, respectively by aligning raw data to the start of analyte injection and performing subtraction of reference flow cell. Single reference subtracted data from both instruments were later exported as text files and analyzed using the Scrubber fitting model

(version 2.0c, BioLogic Software, Campbell, Australia), wherein a second reference subtraction using control buffer injections was performed, and the double reference subtracted data was globally fitting to a 1:1 Langmuir binding model with mass transport limitation.

3. RESULTS

3.1. Binding Rate Constants Measured Across Different Flow Channels are comparable

Unlike most of the available SPR platforms that utilize a serial flow integrated fluidic cartridge (IFC) design, MASS-1 is an eight-channel parallel flow IFC system. Therefore, before initiating an extensive binding study on MASS-1, we verified the reproducibility of binding rate constants measured for mAbs captured across different flow channels. A total of fifteen mAbs were selected in this study, which were sub-divided into five groups based on the molecular weight of their respective antigen: mAb# 1-3 for 20kD, mAb# 4-6 for 28kD, mAb# 7-9 for 48kD, mAb# 10-12 for 77kD and mAb# 13-15 for 92kD antigen. The same mAb was captured across the eight flow channels of MASS-1, and the association rate (k_a), dissociation rate (k_d), and dissociation constant (K_D) were measured. The results of the kinetic analysis for mAbs captured on different flow channels are provided in Table 1 and the representative real time binding sensorgrams are shown in Figure 2. Comparable binding kinetic values were measured across different flow channels and less than 10% deviation of the measured rate constants was observed for all fifteen mAbs included in this study.

Binding studies for the same set of mAb-antigen interactions were also performed on the Biacore 4000 platform (Table 1). Variability in the binding rate constants measured on different biosensors was assessed by plotting correlation factor determined by calculating the ratio of individual k_a, k_d, and K_D values measured on the Biacore 4000 and different flow channels of MASS-1 as shown in Figure 3. Irrespective of the flow channel used on MASS-1, binding rate constants for all the fifteen mAb-antigen interactions were within three-fold of the values generated using Biacore 4000 and is considered to be within the experimental error of any RT-LF binding study.

Figure 2: Real-time Binding Sensorgrams of mAb Captured Across Different Flow Channels

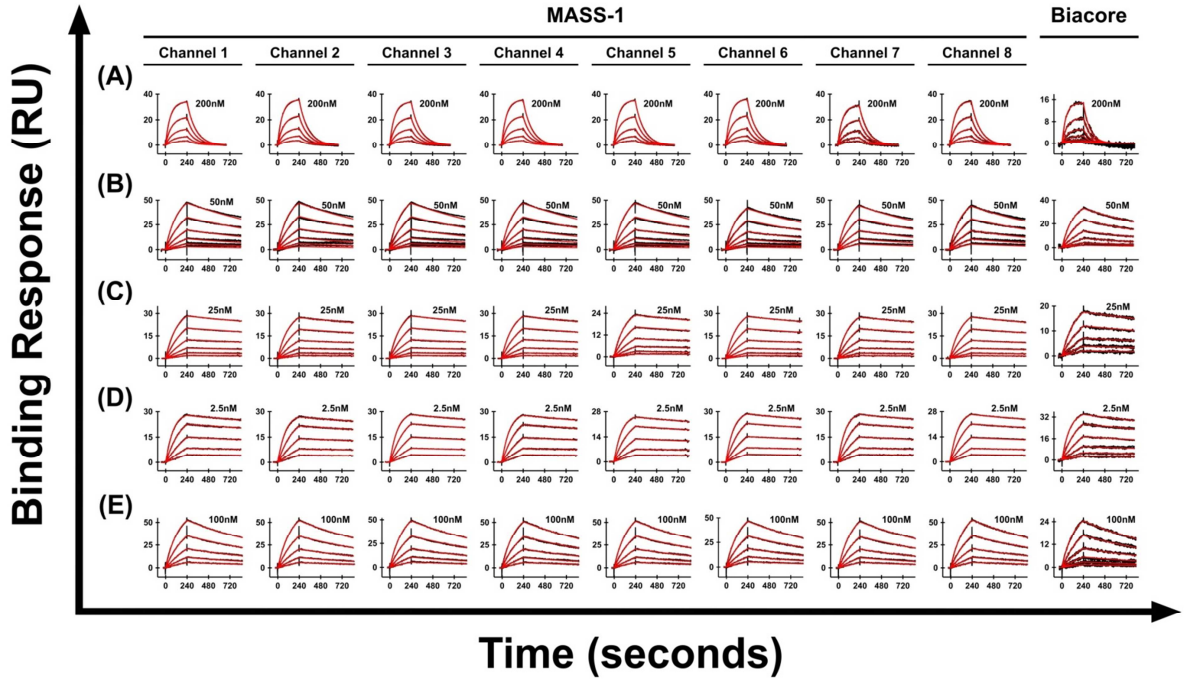

Comparable density of mAb was first captured across different flow channels (Channel-1 through Channel-8) on HCA sensors immobilized with anti-human Fcγ capture mAb. Different concentrations of antigen (serially diluted two-fold) were injected over the mAb capture surface for 4 minutes and dissociation of bound antigen in running buffer was observed for 10 minutes. Real time binding sensorgrams of mAb binding to 20kD **(A)**, 28kD **(B)**, 48kD **(C)**, 77kD **(D)**, and 92kD **(E)** antigen are shown as black lines while red lines represent model fits generated by globally fitting real-time binding data using a 1:1 binding model with mass transport limitation. Binding sensorgrams comprise at least duplicate injections of same antigen concentration. All mAb-antigen binding interactions were also characterized on Biacore 4000 platform under comparable experimental conditions and the binding sensorgrams along with the global fits are presented. Highest antigen concentration used to fit binding data is provided and binding kinetics values generated are provided in Table 1.

Table 1: Binding Kinetics Parameters Determined Across Different Flow Channels of MASS-1 and on Biacore 4000

	mAb Captured	Kinetic Parameters	Channel 1	Channel 2	Channel 3	Channel 4	Channel 5	Channel 6	Channel 7	Channel 8	Average ± Std Dev	Biacore
20kD Antigen	mAb-1	k_a (1/Ms)	4.74E+04	4.84E+04	4.67E+04	4.80E+04	4.74E+04	4.68E+04	4.66E+04	4.83E+04	(4.74 ± 0.07) E+04	4.64E+04
		k_d (1/s)	1.02E-02	1.00E-02	9.97E-03	1.04E-02	1.05E-02	1.00E-02	1.07E-02	9.89E-03	(1.02 ± 0.03) E-03	1.35E-02
		K_D (M)	2.16E-07	2.07E-07	2.13E-07	2.17E-07	2.22E-07	2.14E-07	2.30E-07	2.05E-07	(2.15 ± 0.08) E-07	2.90E-07
	mAb-2	k_a (1/Ms)	7.25E+04	7.58E+04	7.68E+04	7.63E+04	7.24E+04	7.74E+04	6.29E+04	8.41E+04	(7.48 ± 0.60) E+04	7.19E+04
		k_d (1/s)	2.59E-03	2.59E-03	2.56E-03	2.54E-03	2.62E-03	2.53E-03	2.70E-03	2.56E-03	(2.58 ± 0.05) E-03	4.06E-03
		K_D (M)	3.57E-08	3.42E-08	3.33E-08	3.33E-08	3.61E-08	3.27E-08	4.28E-08	3.04E-08	(3.48 ± 0.37) E-08	5.65E-08
	mAb-3	k_a (1/Ms)	1.58E+05	1.76E+05	1.64E+05	1.62E+05	1.56E+05	1.68E+05	1.49E+05	1.64E+05	(1.62 ± 0.08) E+05	1.51E+05
		k_d (1/s)	5.86E-04	5.96E-04	5.93E-04	5.97E-04	5.79E-04	6.02E-04	6.04E-04	6.03E-04	(5.95 ± 0.09) E-04	8.77E-04
		K_D (M)	3.70E-09	3.38E-09	3.62E-09	3.69E-09	3.72E-09	3.58E-09	4.07E-09	3.68E-09	(3.68 ± 0.19) E-09	5.82E-09
28kD Antigen	mAb-4	k_a (1/Ms)	1.39E+06	1.39E+06	1.48E+06	1.44E+06	1.33E+06	1.51E+06	1.36E+06	1.38E+06	(1.41 ± 0.06) E+06	2.52E+06
		k_d (1/s)	3.52E-02	3.35E-02	3.51E-02	3.50E-02	3.54E-02	3.54E-02	3.44E-02	3.27E-02	(3.46 ± 0.10) E-02	7.43E-02
		K_D (M)	2.53E-08	2.40E-08	2.37E-08	2.44E-08	2.67E-08	2.34E-08	2.52E-08	2.37E-08	(2.46 ± 0.11) E-08	2.94E-08
	mAb-5	k_a (1/Ms)	6.65E+05	6.53E+05	6.51E+05	6.64E+05	6.72E+05	6.50E+05	6.68E+05	6.77E+05	(6.62 ± 0.10) E+05	9.94E+05
		k_d (1/s)	2.43E-03	2.46E-03	2.49E-03	2.52E-03	2.48E-03	2.56E-03	2.45E-03	2.45E-03	(2.48 ± 0.04) E-03	2.39E-03
		K_D (M)	3.66E-09	3.76E-09	3.82E-09	3.79E-09	3.69E-09	3.94E-09	3.67E-09	3.61E-09	(3.74 ± 0.11) E-09	2.41E-09
	mAb-6	k_a (1/Ms)	1.43E+05	1.61E+05	1.56E+05	1.52E+05	1.50E+05	1.54E+05	1.51E+05	1.53E+05	(1.52 ± 0.05) E+05	1.48E+05
		k_d (1/s)	6.93E-04	6.93E-04	6.99E-04	6.89E-04	7.22E-04	6.91E-04	7.08E-04	7.05E-04	(7.00 ± 0.11) E-04	7.83E-04
		K_D (M)	4.84E-09	4.31E-09	4.47E-09	4.54E-09	4.83E-09	4.48E-09	4.70E-09	4.61E-09	(4.60 ± 0.18) E-09	5.28E-09
48kD Antigen	mAb-7	k_a (1/Ms)	2.51E+05	2.50E+05	2.53E+05	2.54E+05	2.51E+05	2.39E+05	2.49E+05	2.46E+05	(2.49 ± 0.05) E+05	2.03E+05
		k_d (1/s)	8.87E-04	8.96E-04	8.83E-04	9.14E-04	8.82E-04	8.86E-04	9.09E-04	8.95E-04	(8.94 ± 0.12) E-04	1.04E-03
		K_D (M)	3.53E-09	3.58E-09	3.49E-09	3.60E-09	3.51E-09	3.71E-09	3.65E-09	3.64E-09	(3.59 ± 0.08) E-09	5.12E-09
	mAb-8	k_a (1/Ms)	3.19E+05	3.11E+05	3.11E+05	3.15E+05	3.08E+05	3.01E+05	3.16E+05	3.07E+05	(3.11 ± 0.06) E+05	2.57E+05
		k_d (1/s)	2.09E-04	2.16E-04	2.15E-04	2.20E-04	2.12E-04	2.11E-04	2.07E-04	2.23E-04	(2.14 ± 0.05) E-04	2.82E-04
		K_D (M)	6.56E-10	6.96E-10	6.92E-10	6.99E-10	6.88E-10	7.03E-10	6.54E-10	7.25E-10	(6.89 ± 0.24) E-10	1.10E-09
	mAb-9	k_a (1/Ms)	7.36E+05	7.08E+05	6.85E+05	7.06E+05	6.86E+05	6.80E+05	6.97E+05	6.98E+05	(6.99 ± 0.18) E+05	6.05E+05
		k_d (1/s)	1.21E-04	1.35E-04	1.24E-04	1.52E-04	1.41E-04	1.30E-04	1.40E-04	1.32E-04	(1.34 ± 0.10) E-04	2.12E-04
		K_D (M)	1.65E-10	1.90E-10	1.81E-10	2.15E-10	2.05E-10	1.92E-10	2.01E-10	1.90E-10	(1.92 ± 0.15) E-10	3.50E-10
77kD Antigen	mAb-10	k_a (1/Ms)	5.74E+06	5.53E+06	5.83E+06	5.48E+06	5.58E+06	5.25E+06	5.29E+06	6.13E+06	(5.60 ± 0.29) E+06	4.63E+06
		k_d (1/s)	1.88E-04	1.66E-04	1.65E-04	1.83E-04	1.78E-04	1.84E-04	1.79E-04	1.85E-04	(1.78 ± 0.09) E-04	2.53E-04
		K_D (M)	3.27E-11	2.99E-11	2.83E-11	3.34E-11	3.19E-11	3.50E-11	3.39E-11	3.02E-11	(3.19 ± 0.23) E-11	5.45E-11
	mAb-11	k_a (1/Ms)	1.10E+06	1.04E+06	1.06E+06	1.07E+06	1.03E+06	1.06E+06	1.03E+06	1.06E+06	(1.06 ± 0.02) E+6	6.68E+05
		k_d (1/s)	1.39E-04	1.46E-04	1.40E-04	1.33E-04	1.37E-04	1.40E-04	1.44E-04	1.43E-04	(1.40 ± 0.04) E-04	2.53E-04
		K_D (M)	1.26E-10	1.41E-10	1.32E-10	1.24E-10	1.33E-10	1.32E-10	1.39E-10	1.35E-10	(1.33 ± 0.06) E-10	3.79E-10
	mAb-12	k_a (1/Ms)	1.90E+06	1.86E+06	1.91E+06	1.90E+06	1.89E+06	1.87E+06	1.89E+06	1.80E+06	(1.88 ± 0.04) E+06	1.26E+06
		k_d (1/s)	1.60E-04	1.62E-04	1.65E-04	1.55E-04	1.53E-04	1.75E-04	1.54E-04	1.80E-04	(1.63 ± 0.10) E-04	2.46E-04
		K_D (M)	8.42E-11	8.73E-11	8.64E-11	8.14E-11	8.08E-11	9.32E-11	8.15E-11	1.00E-10	(8.69 ± 0.68) E-11	1.95E-10
92kD Antigen	mAb-13	k_a (1/Ms)	1.34E+05	1.36E+05	1.42E+05	1.45E+05	1.37E+05	1.28E+05	1.42E+05	1.22E+05	(1.36 ± 0.08) E+05	1.52E+05
		k_d (1/s)	1.33E-02	1.29E-02	1.35E-02	1.32E-02	1.36E-02	1.35E-02	1.32E-02	1.33E-02	(1.33 ± 0.02) E-02	1.60E-02
		K_D (M)	9.89E-08	9.49E-08	9.54E-08	9.09E-08	9.93E-08	1.06E-07	9.35E-08	1.09E-07	(9.85 ± 0.63) E-08	1.05E-07
	mAb-14	k_a (1/Ms)	6.76E+04	7.20E+04	6.95E+04	7.27E+04	6.79E+04	6.95E+04	6.94E+04	7.02E+04	(6.98 ± 0.18) E+04	7.19E+04
		k_d (1/s)	7.33E-04	7.10E-04	7.25E-04	7.10E-04	7.66E-04	7.34E-04	7.25E-04	7.32E-04	(7.29 ± 0.18) E-05	8.48E-04
		K_D (M)	1.08E-08	9.87E-09	1.04E-08	9.76E-09	1.13E-08	1.06E-08	1.05E-08	1.04E-08	(1.05 ± 0.05) E-08	1.18E-08
	mAb-15	k_a (1/Ms)	8.71E+04	9.21E+04	9.05E+04	9.34E+04	8.56E+04	8.67E+04	9.03E+04	8.60E+04	(8.90 ± 0.30) E+04	6.78E+04
		k_d (1/s)	1.57E-04	1.55E-04	1.54E-04	1.56E-04	1.69E-04	1.58E-04	1.60E-04	1.68E-04	(1.60 ± 0.06) E-04	1.22E-04
		K_D (M)	1.80E-09	1.68E-09	1.70E-09	1.66E-09	1.98E-09	1.82E-09	1.77E-09	1.95E-09	(1.80 ± 0.12) E-09	1.80E-09

Figure 3: **Correlation Plots of Binding Kinetics Parameters Determined Across Different Flow Channels of MASS-1**

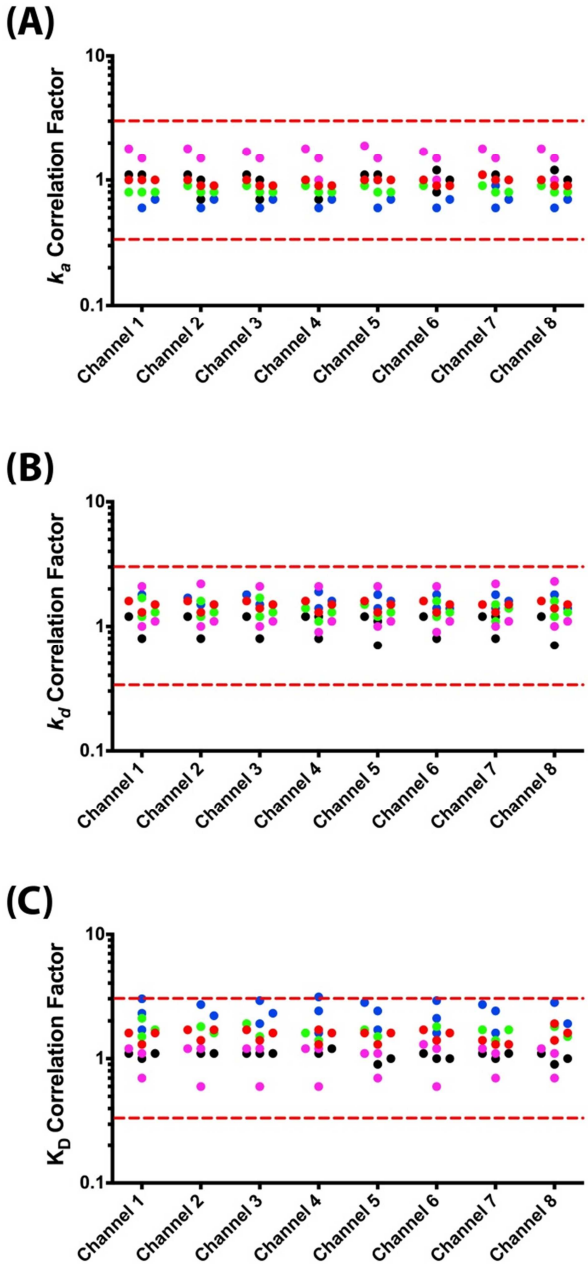

Correlation factor was determined by calculating the ratio of kinetics values measured on Biacore 4000 to those determined on MASS-1 for mAbs captured across different flow channels. Correlation factor calculated for k_a **(A)**, k_d **(B)** and K_D **(C)** measured across different flow channels of MASS-1 for mAb binding to 20kD (●), 28kD (●), 48kD (●), 77kD (●), and 92kD (●) antigen are plotted. Serrated red lines indicate a three-fold difference in the kinetic values with a correlation factor of 3 and 0.33.

3.2. Single Injection Cycle Kinetics Assay is a Reliable Assay that Enhances MASS-1 Throughput

As minimal deviation was observed for binding studies performed across the eight flow channels, MASS-1 provides an opportunity to design kinetics titration assay using the SICK method. Figure 4 provides the schematic of designing SICK assay on MASS-1. A similar level of mAb capture level across all of the eight channels is a pre-requisite for adopting the SICK assay. The mAb can be either immobilized across different flow channels or captured using a relevant capture molecule. Once desirable mAb surface density is attained, different analyte concentrations are simultaneously injected across all eight flow channels, enabling kinetic measurements in two cycles. This reduces experimental time by up to 80% compared to the standard, multiple injection titration kinetics assay format (also referred as MICK assay). Moreover, the SICK assay provides a simpler solution to characterize binding interactions that fail to regenerate and/or are detrimental to the activity of ligand surface. Since optimization of the regeneration condition is not required, the SICK assay can reduce the time to results.

To examine the robustness of the SICK assay format, we included eight different molecular weight antigens with two mAbs per antigen in this study (Figure 5). Reliability of kinetic values was determined by characterizing the same interactions using the standard MICK assay on both MASS-1 and Biacore 4000 (Figure 5). Binding kinetic values measured under the different experimental formats on both biosensors are tabulated in Table 2. Fitted data for all of the binding interactions characterized using different assay formats overlaid with the experimental data. The k_a (Figure 6A and Figure 6D), k_d (Figure 6B and Figure 6E) and K_D (Figure 6C and Figure 6F) values measured using SICK and MICK assay formats were within two-fold of each other for all sixteen mAb-antigen interactions characterized in this study.

Figure 4: Schematic of SICK Assay Design on MASS-1

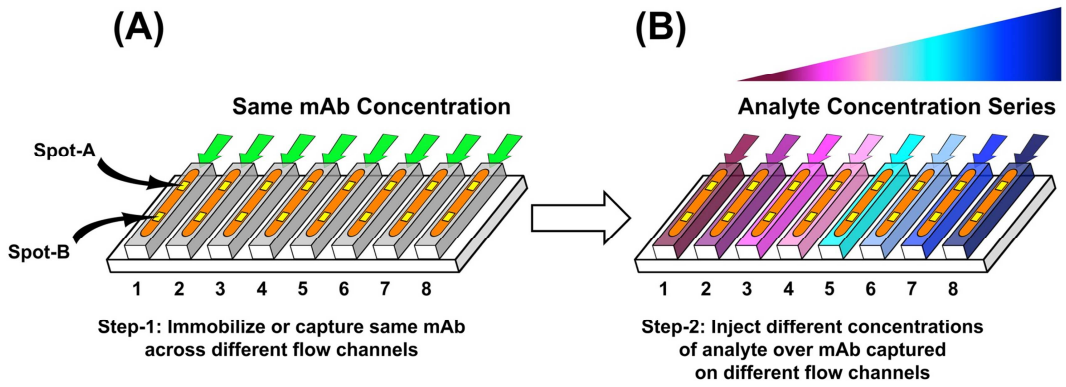

The same mAb is first captured across flow channels 1 through 8 **(A)** followed by the injection of eight concentration series of analyte over mAb captured surfaces **(B)**. Binding rate constants are measured by running two cycles – buffer injection cycle (for second reference subtraction) followed by the injection of eight concentration titers of analyte.

Figure 5: Comparison of MICK and SICK Assays Performed on Different SPR Platforms

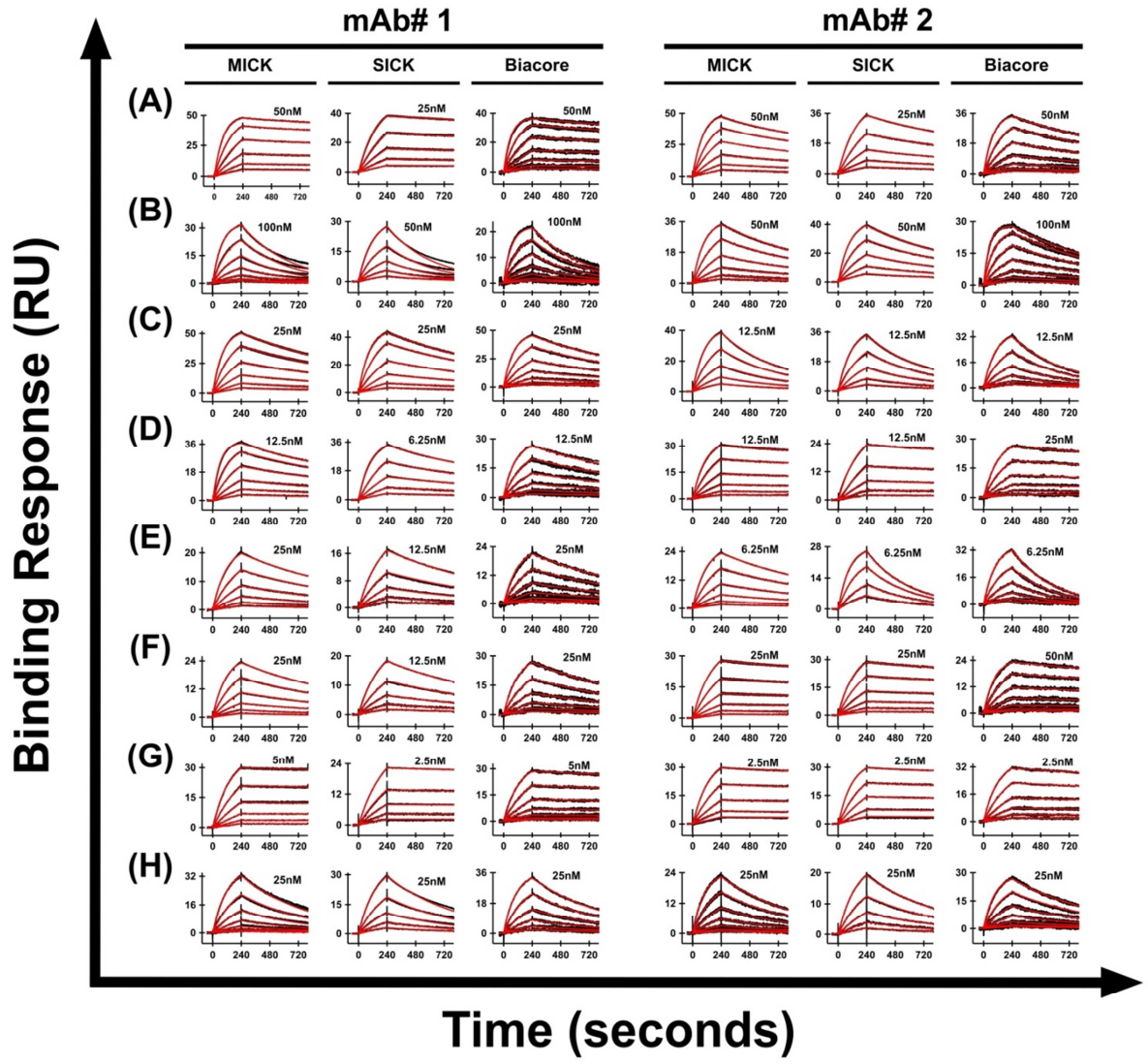

mAb binding to 14kD **(A)**, 18kD **(B)**, 28kD **(C)**, 29kD **(D)**, 38kD **(E)**, 48kD **(F)**, 77kD **(G)**, and 105kD **(H)** antigen was first captured either following SICK assay format on MASS-1 or using the standard MICK assay format on both MASS-1 and Biacore 4000. Two mAbs per antigen were included in this study referred as mAb# 1 & mAb# 2. Different concentrations of antigen serially diluted by two-fold were injected for 4 minutes followed by 10 minutes of dissociation. Overlay of at least triplicate injections of the same antigen concentration is shown in black lines while red lines represent global fits of real-time binding data. The highest concentration used to fit data is shown and kinetics values measured using SICK and MICK assay formats are provided in Table 2. To ensure that our analysis did not introduce any unintended biasing in the measurement of rate constants, all of the binding data generated using the SICK or MICK assay formats on Biacore 4000 and MASS-1 were independently analyzed by adopting the "blind analysis" technique. During the analysis, the antigen concentrations that yielded the best global fits of the double reference subtracted data were selected. This resulted in the incorporation of different antigen concentrations for few interactions as shown in the figure. However, this discrepancy in antigen concentrations used to fit the data did not influence the values of measured kinetics parameters (Table 2).

Table 2: Binding Kinetic Parameters from MICK and SICK Assays Performed on Different SPR Platforms

		MICK Assay			SICK Assay			Biacore 4000 Assay		
Antigen Molecular Weight	mAb Captured	k_a (1/Ms)	k_d (1/s)	K_D (M)	k_a (1/Ms)	k_d (1/s)	K_D (M)	k_a (1/Ms)	k_d (1/s)	K_D (M)
14kD	mAb# 1	3.65E+05	1.52E-04	4.26E-10	2.80E+05	1.36E-04	4.87E-10	3.39E+05	1.96E-04	5.78E-10
	mAb# 2	3.85E+05	6.35E-04	1.66E-09	2.59E+05	5.95E-04	2.29E-09	2.48E+05	7.17E-04	2.89E-09
18kD	mAb# 1	1.05E+05	2.43E-03	2.31E-08	1.20E+05	2.61E-03	2.18E-08	1.32E+05	2.36E-03	1.78E-08
	mAb# 2	1.93E+05	1.02E-03	5.27E-09	2.19E+05	1.06E-03	4.85E-09	2.02E+05	1.12E-03	5.52E-09
28kD	mAb# 1	4.70E+05	7.88E-04	1.68E-09	5.11E+05	8.67E-04	1.71E-09	4.68E+05	8.50E-04	1.82E-09
	mAb# 2	8.63E+05	2.03E-03	2.36E-09	8.62E+05	2.16E-03	2.51E-09	7.19E+05	2.28E-03	3.17E-09
29kD	mAb# 1	1.32E+06	7.00E-04	5.31E-10	2.20E+06	8.50E-04	4.11E-10	9.35E+05	7.72E-04	8.26E-10
	mAb# 2	7.29E+05	1.84E-04	2.52E-10	7.54E+05	1.55E-04	2.16E-10	4.85E+05	1.95E-04	4.03E-10
38kD	mAb# 1	3.13E+05	9.15E-04	2.93E-09	3.43E+05	9.24E-04	2.69E-09	3.00E+05	9.96E-04	3.32E-09
	mAb# 2	2.98E+06	3.60E-03	1.31E-09	2.16E+06	3.21E-03	1.49E-09	1.22E+06	3.03E-03	2.48E-09
48kD	mAb# 1	3.46E+05	8.80E-04	2.54E-09	3.78E+05	8.95E-04	2.37E-09	2.76E+05	9.46E-04	3.43E-09
	mAb# 2	3.28E+05	1.75E-04	5.34E-10	3.05E+05	1.85E-04	6.07E-10	2.07E+05	2.13E-04	1.03E-09
77kD	mAb# 1	1.40E+06	4.70E-05	3.35E-11	2.07E+06	4.91E-05	2.51E-11	1.54E+06	9.45E-05	6.14E-11
	mAb# 2	2.98E+06	1.02E-04	3.43E-11	3.30E+06	9.01E-05	2.76E-11	3.30E+06	1.57E-04	4.75E-11
105kD	mAb# 1	2.65E+05	1.70E-03	6.44E-09	2.11E+05	1.64E-03	7.76E-09	3.40E+05	1.53E-03	4.50E-09
	mAb# 2	3.74E+05	1.55E-03	4.15E-09	2.57E+05	1.56E-03	6.05E-09	3.75E+05	1.37E-03	3.66E-09

Figure 6: Correlation of Binding Kinetic Values Generated Using SICK and MICK Assay Formats on MASS-1 and MICK Assay Format on Biacore 4000

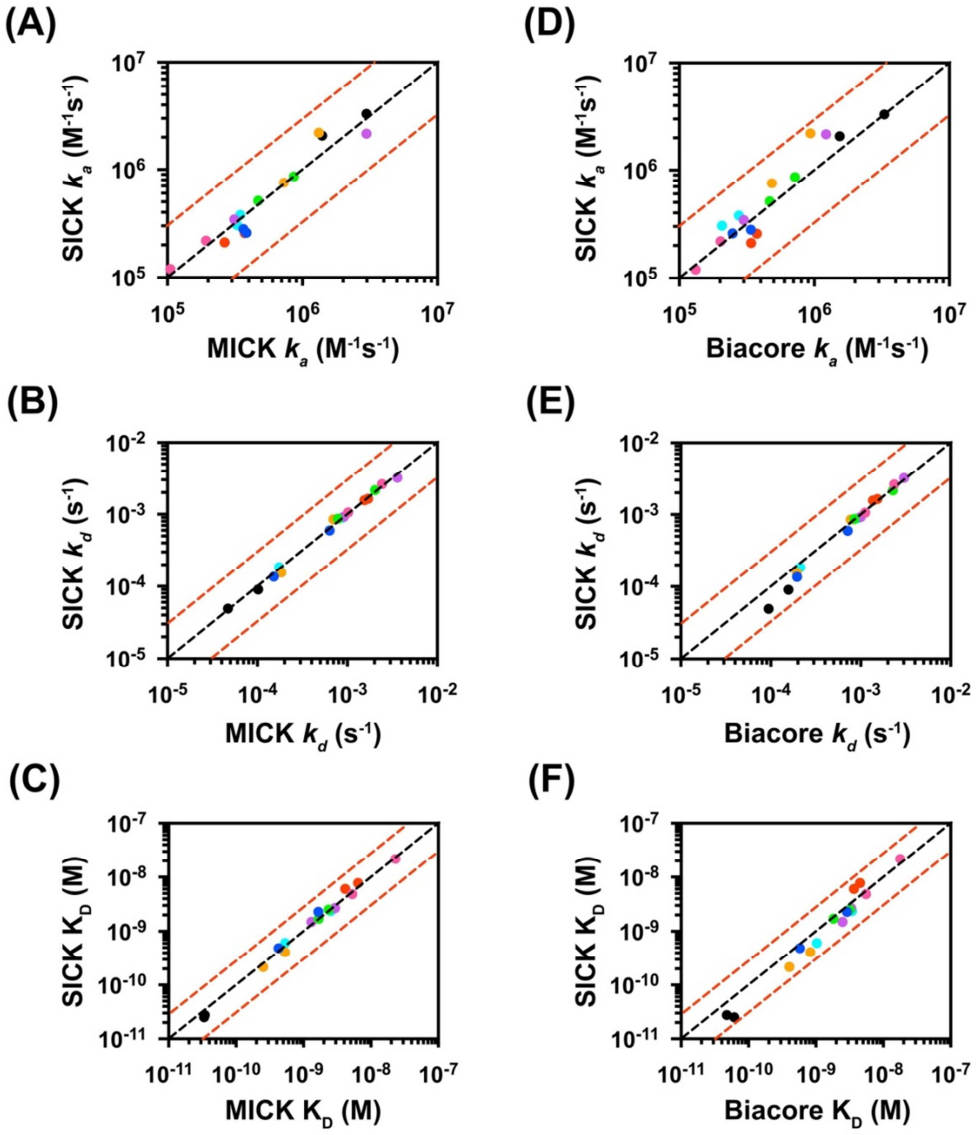

Scatterplot showing correlation between k_a **(A)**, k_d **(B)** and K_D **(C)** values measured using SICK and MICK assay formats on MASS-1 platform for mAbs binding to 14kD (●), 18kD (●), 28kD (●), 29kD (●), 38kD (●), 48kD (●), 77kD (●), and 105kD (●) antigen is shown. Also plotted is correlation between k_a **(D)**, k_d **(E)** and K_D **(F)** values measured using SICK assay on MASS-1 biosensor and MICK assay performed on Biacore 4000. Serrated black line signifies correlation coefficient of 1 while serrated red lines indicate three-fold difference in kinetic values for mAbs binding to different molecular weight antigens.

3.3. Intrinsic Noise of MASS-1 is Independent of Protein Immobilization Level

Initial kinetic assays provided us enough confidence on the reproducibility of the binding rate constants measured on MASS-1 and encouraged us to further understand factors that can affect the noise and sensitivity of MASS-1. The CMOS camera of the MASS-1 detector differs from the linear diode detector of Biacore instruments and utilizes a two-dimensional sensing surface to measure changes in the intensity of the reflected light (14,17). It is known that EDC/NHS surface chemistry results in a non-uniform immobilization of protein on the sensor surface, and thus can potentially interfere with the detection of the reflected light in the MASS-1 (18). Furthermore, we wanted to better understand whether high protein surface densities (greater than 1000RU) influence instrument noise and sensitivity which in turn would limit the application of MASS-1 in designing sensitive kinetic assays with binding response of less than 5RU. In order to achieve this, we needed to (i) perform kinetic assays with protein immobilization levels varying from 500 RU to 10,000RU, and (ii) design binding studies that demonstrate a low signal-to-noise ratio with maximum analyte binding response (R_{max}) value of less than 6RU. We could have captured mAbs at varying densities, but it would have resulted in a corresponding increase in the measured binding response, making it challenging to assess the noise and sensitivity of MASS-1. Moreover, we were also interested in evaluating the reproducibility of the binding curves measured at such low binding signal along with the reliability of kinetic values generated at varying protein density surfaces.

We therefore opted for a simplistic approach of immobilizing different levels of anti-human Fcγ capture molecule (400RU, 1000RU, 2500RU and 10000RU) across different flow channels (**Supplementary Figure S1**). A total of five mAbs binding to antigens with molecular weights of 14kD, 18kD, 28kD, 29kD and 39kD were evaluated (Figure 7). The desired capture level of mAb was achieved by varying the concentration and capture time to achieve an R_{max} of 3-6RU. Varying concentrations of specific antigen (serially diluted by two-fold in running buffer) were injected over mAb captured surface.

Double reference subtracted binding sensorgrams (Figure 7) were visually inspected and no noticeable difference in instrument noise was observed between the different density capture surfaces. The measurements were reproducible, as the sensorgrams for triplicate injections of same antigen concentration showed a good overlay. Moreover, binding rate constants measured for mAbs captured at different anti-human Fcγ density surfaces were found to be within two-fold of each other (Table 3).

Experiments were initially designed to achieve R_{max} of around 5-6 RU for 14kD, 18kD, 28kD and 29kD antigens. Based on the binding data generated for these antigens, mAb capture level was further reduced to achieve R_{max} of approximately 2-3RU for the characterization of the 39kD antigen (Figure 7E**)**. Interestingly, even with such ultra-low density mAb surfaces, we did not observe any increased noise in the real-time binding data generated from 10,000 RU anti-human Fcγ surface. These results demonstrate that neither instrument sensitivity nor measured rate constants were affected by protein density level and based on the visual inspection of the binding data, the instrument noise was found to be around 0.1RU.

Figure 7: Effect of Protein Surface Density on Instrument Noise

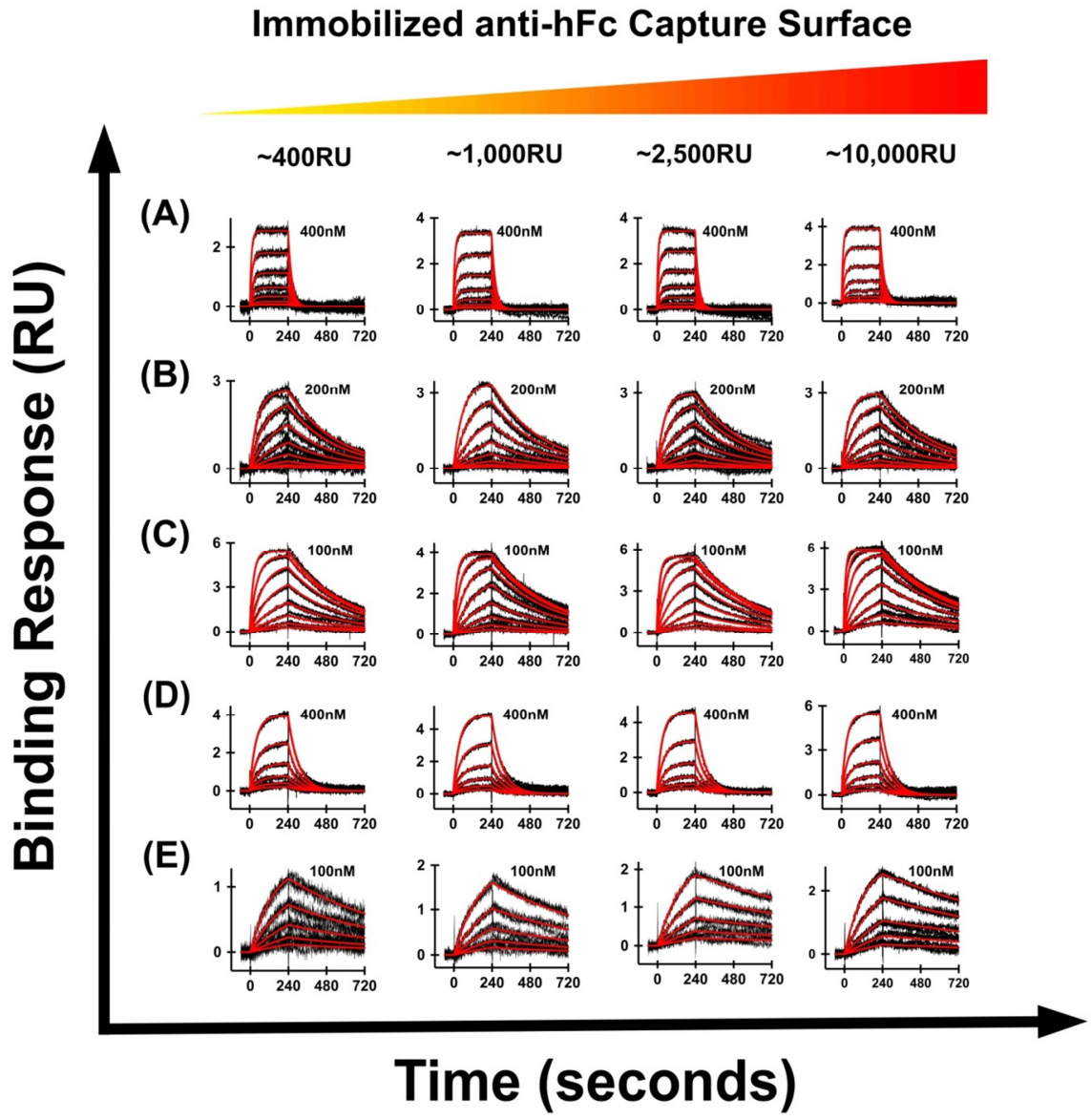

The HCA sensor was first immobilized with different densities of anti-human Fcγ capture mAb (approximately 400RU, 1000RU, 2500RU & 10000RU) using standard EDC-NHS surface chemistry detailed in the Materials and Methods section. A comparable low density of mAb binding to 14kD **(A)**, 18kD **(B)**, 28kD **(C)**, 29kD **(D)**, and 39kD **(E)** antigen was first captured on anti-human Fcγ, immobilized at different surface densities. Varying concentrations of specific antigen (serially diluted by two-fold in running buffer) were injected over mAb captured surface for 4 minutes followed by 10 minutes of dissociation step. Real-time binding of triplicate injections of similar antigen concentration binding to captured mAb is shown in black while global fits generated to calculate kinetics values are shown in red. The highest antigen concentration used to fit binding data is provided and binding kinetics parameters are tabulated in Table 3.

Table 3: Binding Kinetic Parameters Measured using Different Protein Surface Densities

		anti-hFc Immobilization Level			
Antigen Molecular Weight	Kinetics Parameters	400RU	1,000RU	2,500RU	10,000RU
14kD	k_a (1/Ms)	1.48E+05	1.52E+05	2.12E+05	1.85E+05
	k_d (1/s)	4.14E-02	4.09E-02	4.44E-02	3.95E-02
	K_D (M)	2.80E-07	2.69E-07	2.10E-07	2.13E-07
18kD	k_a (1/Ms)	8.61E+04	7.35E+04	1.03E+05	1.01E+05
	k_d (1/s)	3.34E-03	3.25E-03	3.25E-03	3.11E-03
	K_D (M)	3.87E-08	4.42E-08	3.17E-08	3.08E-08
28kD	k_a (1/Ms)	4.11E+05	4.62E+05	5.32E+05	8.12E+05
	k_d (1/s)	2.80E-03	2.66E-03	2.70E-03	2.35E-03
	K_D (M)	6.81E-09	5.75E-09	5.08E-09	2.89E-09
29kD	k_a (1/Ms)	2.80E+04	2.75E+04	3.10E+04	4.29E+04
	k_d (1/s)	1.53E-02	1.52E-02	1.68E-02	1.62E-02
	K_D (M)	5.47E-07	5.52E-07	5.43E-07	3.76E-07
39kD	k_a (1/Ms)	1.07E+05	1.04E+05	1.53E+05	1.63E+05
	k_d (1/s)	1.35E-03	1.24E-03	9.15E-04	9.04E-04
	K_D (M)	1.26E-08	1.20E-08	5.97E-09	5.55E-09

3.4. Sensitivity of MASS-1 Overcame Mass Transport Limitation and Enabled Characterization of High Affinity mAb-antigen Interactions with k_a Values Greater than 10^6 $M^{-1}s^{-1}$

Picomolar affinity interactions typically exhibit slow dissociation rates and/or fast association rates and reliable measurement of binding rate constants for such interactions using an RT-LF platform continues to be a challenge. Analyte binding for picomolar affinity interactions with a k_a value greater than 10^6 $M^{-1}s^{-1}$ is typically limited by diffusion of the analyte from the unstirred layer into the ligand surface, a phenomenon referred to as MTL. The effects of MTL are especially magnified during the association phase when the rate of analyte diffusion is slower than the k_a of the interaction, resulting in a linear binding curve during the association phase (19,20). Furthermore, rebinding of the analyte to the unoccupied ligand on the sensor surface during the dissociation phase is also observed in MTL. Although incorporation of the mass transport constant (k_m) into the two-compartment fitting model enables correction for observed MTL effects, the reliability of binding rate constants measured using this model depends on the magnitude of mass transport (21). Therefore designing kinetics assay devoid of any MTL is highly recommended to generate reliable k_a, k_d, and K_D values of any biomolecular interactions.

One of the primary sources of MTL is the concentration gradient of the injected analyte caused by the laminar flow of injected samples in a microfluidic device such as Biacore and MASS-1 (20,22,23). Although increasing flow rate reduces MTL, the value of k_m depends on $1/3^{rd}$ the power of flow rate and necessitates bigger injection volumes and larger sample injection pumps, a technical challenge that is difficult to incorporate in a microfluidic platform (19,20). Therefore, reducing ligand surface density is the preferred choice for kinetic analysis to address MTL

(21,24). Because we observed that MASS-1 generates reproducible binding data even using ultra-low density mAb surfaces (Figure 7), we evaluated its ability to characterize high affinity, MTL-limited mAb-antigen interactions. Moreover, we wanted to demonstrate that measurement of picomolar affinity interactions using SPR/SPRi is not limited by the molecular weight of the analyte. We therefore selected three mAbs to 97kD, 14kD and 3.5kD antigens that did not exhibit MTL with R_{max} of less than 8RU. Using anti-human Fcγ capture surface, mAb was first captured at four different surface densities as indicated in Figure 8 and varying antigen concentrations were injected. Results of the kinetic analysis are provided in Table 4.

Experimental evidence of mass transport effect was demonstrated by normalizing real-timing binding data to the observed experimental R_{max} (Figure 8D-F). We visually examined the shape of the binding sensorgrams generated using different density mAb surfaces, and interpreted that MTL was the dominant feature for all the 3 antigens studied using highest density mAb surface.

The association phase of 97kD and 14kD antigens binding to the highest density mAb surface was significantly mass transport limited, and antigen binding failed to demonstrate any curvature for the 97kD (Figure 8D) and 14kD (Figure 8E) antigens. As the mAb surface density was reduced, a non-linear association binding curve was observed. No substantial increase in the curvature of binding signal was observed once the mAb surface density was below 13RU and 35RU for the 97kD and 14kD antigens, respectively, indicating that the binding interaction was no longer limited by mass transport (Figure 8D-E). These findings were not surprising, since the kinetic assay was designed to only exhibit MTL at the highest density mAb surface.

Although the association phase of the 3.5kD antigen binding data was less sensitive to the mAb surface density, reduced dissociation rate was observed with increasing mAb density (Figure 8F), suggesting that antigen binding to the 320RU mAb surface was also affected by MTL. This disparity in the observed mass transport limitation behavior can be attributed to the differences in the binding kinetic profiles for all three antigens. Unlike the 97kD and 14kD antigens, the 3.5kD antigen has a much faster k_d and hence the interaction reached binding equilibrium faster than 97kD and 14kD antigens. Therefore, a non-linear binding curve was observed during the association phase of 3.5kD antigen. On the other hand, the inherent fast dissociation rate of 3.5kD antigen resulted in its rebinding to the unoccupied mAb on the surface, thereby artificially reducing the dissociation rate for the higher mAb density surface. Similar analyte rebinding can be anticipated for 97kD and 14kD antigens at higher mAb surface densities under mass transport limited conditions. However, since both the antigens exhibit slower k_d than the 3.5kD antigen, a much longer dissociation time would be required to observe such rebinding behavior.

The MTL observed at highest density mAb surfaces is further supported by the k_m values generated by the fitting model. Lower k_m values indicate higher dominance of mass transport in a particular interaction. An inverse correlation was observed between k_m values generated by the fitting model and mAb surface density Table 4, which suggest that the binding interaction was limited by the rate of diffusion of the antigen into the mAb surface. Although all three mAb-antigen interactions showed MTL at the highest mAb densities, the mass transport limited model was able to appropriately compensate for observed MTL, and similar k_a, k_d, and K_D values were generated for all mAb density surfaces. Exclusion of k_m from the fitting model however, yielded poor fits for antigen binding to high density mAb surfaces (Supplementary Figure S2) with high residuals (the difference between experimental data and calculated fits) as shown in Supplementary Figure S2. A systematic 3-4RU residuals were observed for the highest density

mAb surfaces for14kD and 97kD antigens and the measured k_a values were underestimated (Supplementary Table I). However, the same model successfully fitted binding data generated using lowest density mAb surfaces (Supplementary Figure S2). Minimal residuals for the two lower mAb densities for the 14kD and 3.5kD antigens and for the 4RU mAb surface for the 97kD antigen was observed with a random distribution profile around 0RU, which is characteristic of a good fit. Moreover, similar binding kinetic values were measured for these density surfaces irrespective of inclusion or exclusion of k_m factor in the fitting model (Supplementary Table I).

Figure 8: Characterization of High Affinity mAb-antigen Interactions by Circumventing MTL

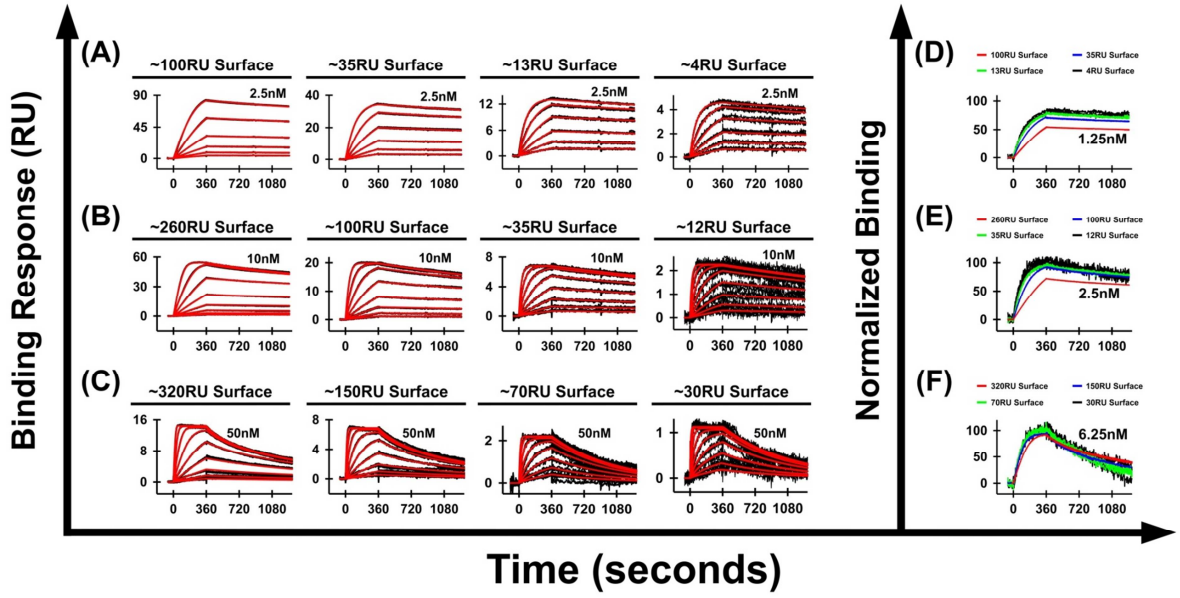

Different levels of mAb to 97kD **(A, D)**, 14kD **(B, E)**, and 3.5kD **(C, F)** antigen were first captured using anti-human Fcγ as indicated. Varying concentrations of antigen (two-fold serial dilution in running buffer) were injected over different mAb surfaces for 6 minutes followed by 15 minutes dissociation. The overlay of triplicate injections of each antigen concentration is shown as black lines and global fitting of real time binding data using 1:1 binding model with mass transport limitation is shown in red. The highest antigen concentration used to fit binding data is also shown and the calculated binding kinetics values are tabulated in Table 4. Binding response observed for 97kD **(D)**, 14kD **(E)**, and 3.5kD **(F)** antigen at indicated concentration was normalized based on the maximum binding signal (R_{max}) observed for respective mAb surface densities to demonstrate MTL. Since the binding curve for 14kD antigen was significantly dominated by MTL when the 260RU surface was used for measurement, we experienced difficulty in fitting the binding data even after incorporating k_m in the fitting model (data not shown). The default initial k_m value of 10^{10} used by the Scrubber fitting software yielded erroneous kinetic values and hence the initial k_m value had to be empirically changed to generate the fits shown in **B.**

Table 4: Binding Parameters for High Affinity Interactions Measures on MASS-1

		Kinetics Parameters			
Antigen Molecular Weight	mAb Capture Level (RU)	k_m (1/Ms)	k_a (1/Ms)	k_d (1/s)	K_D (M)
97kD	100	2.38E+08	5.29E+06	1.53E-04	2.89E-11
	35	4.86E+08	4.68E+06	1.18E-04	2.52E-11
	13	1.00E+10	5.30E+06	1.07E-04	2.02E-11
	4	1.00E+10	5.68E+06	1.28E-04	2.26E-11
14kD	260	7.46E+07	3.38E+06	3.09E-04	9.13E-11
	100	9.79E+07	3.77E+06	2.65E-04	7.03E-11
	35	1.00E+10	3.81E+06	2.28E-04	5.98E-11
	12	1.00E+10	5.30E+06	2.66E-04	5.00E-11
3.5kD	320	1.02E+07	1.59E+06	1.50E-03	9.43E-10
	150	1.49E+07	2.94E+06	1.85E-03	6.27E-10
	70	1.59E+08	1.80E+06	1.40E-03	7.73E-10
	30	1.00E+10	1.56E+06	1.50E-03	9.57E-10

3.5. Comparability Study of a Panel of 189 mAbs Demonstrates Concordance Between Data Generated Using MASS-1 and Biacore 4000

Based on the data presented in Figures 2 through Figure 8, it is evident that the MASS-1 is a sensitive, high-throughput SPRi biosensor capable of measuring reliable binding rate constants. However, in order to incorporate MASS-1 into Regeneron's secondary screening workflow, it was important for us to understand the complexity involved in setting up high-throughput kinetic screening assays to rapidly characterize a panel of 30-40 purified mAbs binding to the target antigen. Moreover, we were interested in evaluating the reliability of kinetic values measured under such high-throughput kinetic screening mode. We therefore performed kinetic analysis on a panel of 189 human mAbs to antigens with molecular weights ranging from 14kD to 105kD. Eight out of thirteen antigens selected in this comparability study (14kD, 28kD, 29kD, 38kD, 48kD, 77kD, 92kD and 105kD) were also used in the previous studies (**Figure 2**, **Figure 5**, **Figure 7** and **Figure 8**).

Multiple cycle titration kinetic assays were performed to measure binding rate constants by first capturing mAb on an anti-human Fcγ immobilized surface and later injecting different concentrations of antigen for 4 minutes followed by a 10 minute dissociation phase. Representative binding curves for mAb binding to 14kD, 21kD, 29kD, 48kD, 77kD, and 97kD antigens are shown in Figure 9, and their respective average kinetic values generated from three independent experiments (± standard deviation) are provided in Table 5. During the analysis of slow dissociating mAb-antigen interactions, we did not observe any significant change in the binding response under the high-throughput experimental format. Extending the dissociation time would have enabled us to reliably determine k_d value of such interactions. Since the aim of this study was to evaluate the performance of MASS-1 under high-throughput screening mode, extending the dissociation time was beyond the scope of this comparability study. To observe at least 5% change in the binding response during the dissociation time of 10 minutes as recommended previously (25), the noise and sensitivity of MASS-1 and Biacore 4000 would

only allow the measurement of the k_d value up to $5x10^{-5}$ s^{-1}. Therefore during the analysis, the k_d values of the interactions for which we did not observe any dissociation of the antigen from the antibody surface were manually fixed to the limitation of the kinetic assay ($5x10^{-5}$ s^{-1}).

Figure 10 provides the scatterplot showing the correlation of average binding kinetic parameters determined from three independent experiments for all 189 mAbs measured on Biacore 4000 and MASS-1. The values of measured rate constants for all 189 mAb-antigen interactions are also listed in **Supplementary Table II**. Approximately 98% of the k_a values were found to be within two-fold of each other, while approximately 90% and 96% of the measured k_d values were two-fold and three-fold of each other, respectively. Approximately 76% of the K_D values measured using MASS-1 and Biacore 4000 were found to be within two-fold of each other, while 95% were within three-fold. Although binding studies were performed under similar experimental conditions, we observed approximately 4% - 5% of the measured k_d and K_D values to be outliers in the correlation plots. Based on the visual inspection of correlation plots, we did not observe any systematic trend in the measured k_a values as reported earlier (15) and the mean ratio of the k_a values measured on Biacore 4000 to MASS-1 was found to be 1. However, a systematic trend in the k_d values was observed and the binding dissociation rates measured on MASS-1 were found to be approximately 1.5 fold lower than those measured on Biacore 4000. This trend resulted in similar fold difference in the K_D values.

Figure 9: Representative Binding Sensorgrams from Comparability Study

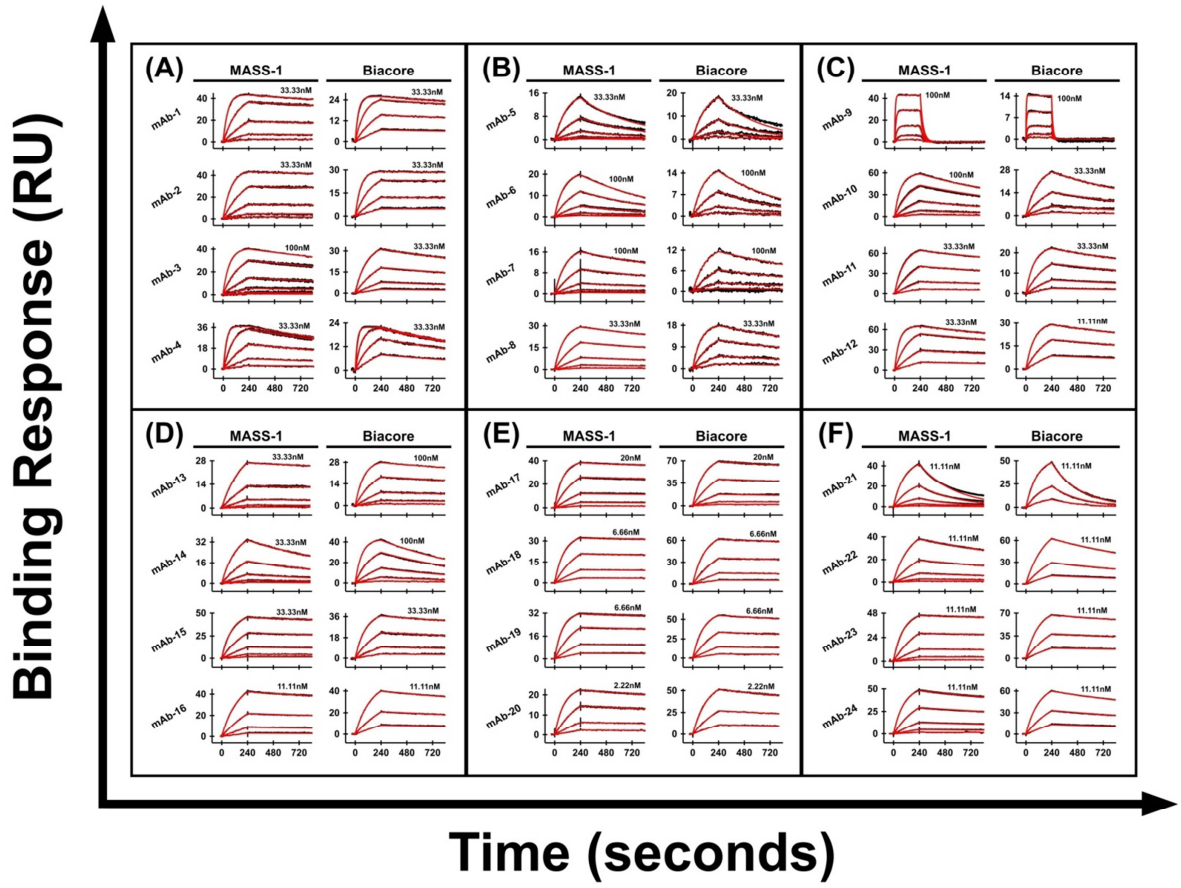

Depending on the molecular weight of the antigen, different levels of mAb binding to 14kD (A), 21kD (B), 29kD (C), 48kD (D), 77kD (E), and 97kD (F) antigen was captured using anti-human Fcγ followed by injection of different concentrations of antigen serially diluted by three-fold. To avoid non-specific binding of 30kD antigen, kinetic studies were performed in HBS-ET running buffer supplemented with 450mM sodium chloride (final concentration). Real time binding sensorgrams of duplicate injection for same antigen concentration is shown in black. The highest antigen concentration used to fit binding data is provided. Global fits obtained using 1:1 binding model with mass transport limitation is represented by red lines and calculated binding kinetics parameters are tabulated in Table V. "Blind analysis" technique of double reference subtracted binding sensorgrams was performed (as described in Figure 5) and the concentration series used to fit the binding curve generated using MASS-1 and Biacore 4000 were found to be different for few mAb-antigen interactions (mAb-3, mAb-10, mAb-12, mAb-13). However, no significant difference in their respective measured kinetics values was observed.

Table 5: Binding Kinetics Values Generated in the Comparability Study

		Biacore 4000			MASS-1		
Antigen Molecular Weight	mAb Captured	k_a ($1x10^5$ 1/Ms)	k_d ($1x10^{-4}$ 1/s)	K_D ($1x10^{-9}$ M)	k_a ($1x10^5$ 1/Ms)	k_d ($1x10^{-4}$ 1/s)	K_D ($1x10^{-9}$ M)
14kD	mAb-1	10.21 ± 0.25	2.04 ± 0.16	0.20 ± 0.02	7.46 ± 0.92	1.79 ± 0.14	0.24 ± 0.05
	mAb-2	6.12 ± 0.10	0.55 ± 0.39	0.09 ± 0.06	4.17 ± 0.59	0.75 ± 0.12	0.19 ± 0.06
	mAb-3	2.87 ± 0.16	3.83 ± 0.12	1.33 ± 0.04	1.58 ± 0.12	3.41 ± 0.33	2.17 ± 0.29
	mAb-4	15.8 ± 0.50	6.31 ± 0.09	0.40 ± 0.01	10.99 ± 2.27	5.03 ± 0.17	0.47 ± 0.12
21kD	mAb-5	1.65 ± 0.41	25.81 ± 2.61	16.50 ± 5.15	2.71 ± 1.53	22.07 ± 3.86	10.62 ± 6.74
	mAb-6	0.78 ± 0.04	16.27 ± 1.34	20.90 ± 1.92	0.78 ± 0.07	14.00 ± 1.45	18.03 ± 1.46
	mAb-7	0.59 ± 0.09	9.45 ± 1.51	16.47 ± 4.77	0.94 ± 0.20	7.24 ± 2.27	7.61 ± 0.83
	mAb-8	3.30 ± 0.26	5.56 ± 0.85	1.71 ± 0.37	2.88 ± 0.61	4.67 ± 0.97	1.62 ± 0.04
29kD	mAb-9	17.29 ± 5.04	704.00 ± 218.53	40.53 ± 1.12	14.12 ± 1.52	438.40 ± 37.29	31.10 ± 1.51
	mAb-10	2.24 ± 0.42	7.99 ± 0.48	3.68 ± 0.94	2.30 ± 0.52	7.19 ± 0.05	3.25 ± 0.86
	mAb-11	3.42 ± 0.80	4.38 ± 0.35	1.36 ± 0.47	3.88 ± 0.43	2.81 ± 0.10	0.73 ± 0.11
	mAb-12	10.12 ± 2.47	3.49 ± 0.16	0.36 ± 0.12	9.71 ± 2.54	3.09 ± 0.18	0.33 ± 0.08
48kD	mAb-13	1.41 ± 0.17	2.03 ± 0.67	1.44 ± 0.40	1.52 ± 0.23	1.14 ± 0.03	0.76 ± 0.14
	mAb-14	1.79 ± 0.17	9.54 ± 0.69	5.36 ± 0.52	2.07 ± 0.02	7.51 ± 0.21	3.63 ± 0.08
	mAb-15	3.26 ± 0.21	1.98 ± 0.60	0.61 ± 0.21	3.25 ± 0.001	1.09 ± 0.05	0.34 ± 0.02
	mAb-16	5.78 ± 0.75	2.18 ± 0.49	0.38 ± 0.05	6.00 ± 0.12	1.52 ± 0.02	0.25 ± 0.001
77kD	mAb-17	5.07 ± 0.06	1.49 ± 0.08	0.29 ± 0.01	7.06 ± 0.82	0.93 ± 0.05	0.13 ± 0.01
	mAb-18	13.76 ± 0.14	1.04 ± 0.07	0.08 ± 0.001	17.22 ± 0.55	0.59 ± 0.06	0.03 ± 0.001
	mAb-19	16.13 ± 0.41	1.37 ± 0.10	0.08 ± 0.01	20.42 ± 0.91	0.83 ± 0.12	0.04 ± 0.01
	mAb-20	34.81 ± 3.99	2.49 ± 0.13	0.07 ± 0.01	56.19 ± 2.76	1.78 ± 0.05	0.03 ± 0.001
97kD	mAb-21	5.78 ± 0.59	41.66 ± 3.33	7.29 ± 1.28	8.97 ± 2.21	38.37 ± 7.23	4.36 ± 0.65
	mAb-22	4.91 ± 1.27	6.13 ± 0.31	1.31 ± 0.39	5.66 ± 0.36	5.06 ± 0.23	0.90 ± 0.10
	mAb-23	8.13 ± 0.32	1.45 ± 0.38	0.18 ± 0.05	9.78 ± 0.31	0.76 ± 0.07	0.08 ± 0.01
	mAb-24	7.17 ± 0.49	3.66 ± 0.19	0.51 ± 0.03	9.43 ± 0.38	2.74 ± 0.04	0.29 ± 0.02

Figure 10: Correlation Plots of Binding Kinetics Values Generated in the Comparability Study

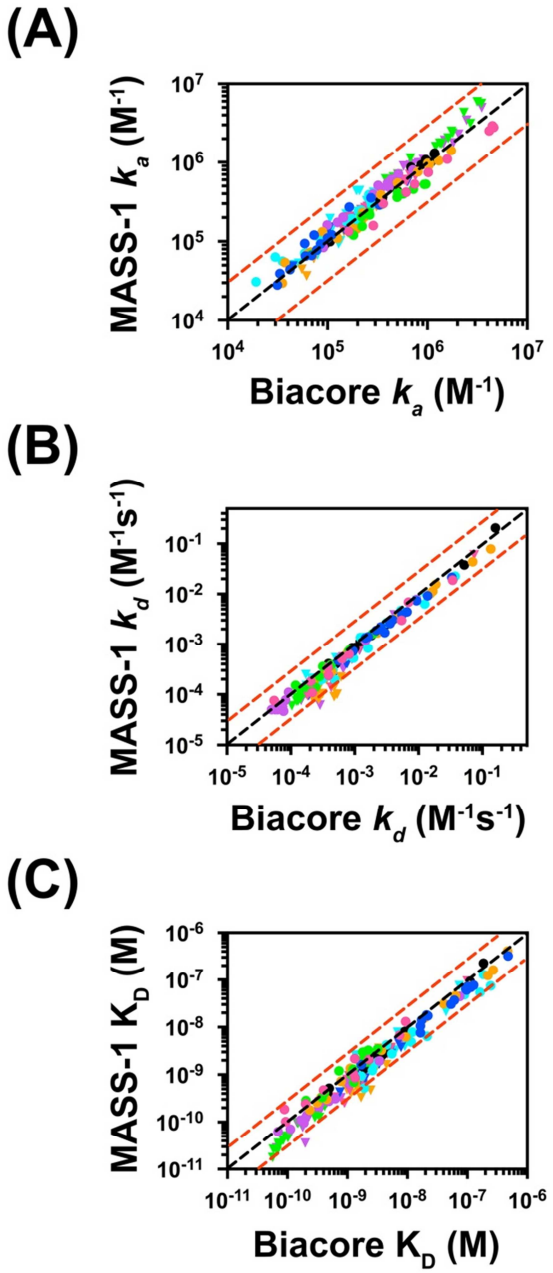

Graphical representation revealing correlation of binding kinetics values measured for 189 mAbs binding to antigens with molecular weights of 14kD (●), 21kD (●), 28kD (●), 29kD (●), 30kD (●), 32kD (●), 38kD (●), 48kD (▼), 68kD (▼), 77kD (▼), 92kD (▼), 97kD (▼), and 105kD (▼) is shown. Scatterplot of average values of k_a **(A)**, k_d **(B)** and K_D **(C)** measured from three independent experiments using Biacore 4000 and MASS-1 is shown. Correlation factor of 1 is shown as serrated black line while three-fold difference in the kinetic values is shown as serrated red line.

4. DISCUSSION

Development of tools capable of screening and characterizing new drug molecules in a high-throughput manner is vital to support the current fast paced biopharmaceutical industry (20). In this work, we evaluated the capability of MASS-1 to characterize mAb-antigen interactions exhibiting varying binding kinetic profiles under diverse assay formats.

The eight channel parallel flow system of MASS-1 provides a new approach for performing kinetic analysis using the SICK assay format presented in this work. One of the key aspects of MASS-1 is its HI technology that uniformly delivers samples across different flow channels of the sensor surface. We routinely immobilize anti-human Fcγ capture molecule on to the sensor surface and less than 4% variability in the immobilization levels are typically observed (data not shown). This enables similar capture level of mAb across different flow channels using the same mAb sample and thus saves experimental time to design SICK assay. Moreover, less than 10% deviation in the binding rate constants measured across different flow channels further provided us enough confidence to perform kinetic analysis using the SICK format on the MASS-1 biosensor.

Conventionally, MICK assays are designed by running multiple cycles, with each cycle generating binding data for an individual analyte concentration. The biggest challenge in such assays is the need to regenerate the sensor surface in between each cycle. The SICK assay overcomes this hurdle by allowing the generation of concentration dependent analyte binding across different flow channels without the need for a regeneration step. We characterized a total of sixteen mAb-antigen interactions, and the kinetic values measured using the SICK assay were within two-fold of the values generated using the traditional MICK assay on Biacore 4000 and MASS-1. A two to three-fold difference in measured binding rate constants is considered to be within acceptable experimental deviation, especially since the measurement of k_a, k_d, and K_D values can be influenced by factors such as sensor surface chemistry, analyte charge, IFC design, and sample delivery system (15,16,26,27). We therefore believe that the observed two-fold difference between SICK and MICK assays is acceptable and that the SICK assay format is a valid approach for kinetic analysis on the MASS-1 biosensor. In our SICK studies, antigens were serially diluted by two-fold and six different antigen concentrations were simultaneously injected over the mAb captured sensor surface. Increasing the antigen dilution factor to three would allow kinetic analysis of two mAbs per cycle (four concentrations per mAb). This would further increase the throughput of SICK assay by two-fold. However, four antigen concentrations might not be enough to characterize mAb panels comprising of a wide range of binding affinities and experiments should be designed with this caveat in mind.

To determine whether the SPRi detection method of MASS-1can limit its applicability to design sensitive kinetic assays with R_{max} of less than 6RU, we designed a series of experiments to test the effects of protein surface density on the instrument noise and accuracy in the measurement of binding kinetic parameters (Figure 7). We found no correlation between protein immobilization level and instrument noise. MASS-1 generated reproducible binding sensorgrams for binding responses of less than 6RU, and triplicate injections of same antigen concentration overlapped. The most intriguing observation was that even under 2RU of binding response, MASS-1 generated reproducible binding sensorgrams (triplicate injections of same antigen concentration showed good overlap) and the instrument sensitivity enabled differentiation of specific signal from noise, irrespective of the surface density of anti-human Fcγ capture molecule. We

understand that mAb-antigen interactions are typically not characterized using high density ligand surfaces, but this observation is an important aspect for the fragment based drug discovery (FBDD). Molecular weight of fragments typically ranges from 150-250 Dalton and researchers aim to immobilize 5,000-10,000 RU of antigen with the hope of observing around 20-40RU of specific binding response. Since the observed specific binding signal is typically low, it is imperative that sensitivity of the biosensors is unaffected by such high density protein surfaces. Since our work shows that irrespective of the immobilized protein surface density, MASS-1 can generate reproducible binding data even for low RU of binding response, overloading the sensor surface with target protein is not required. Moreover, kinetic analysis performed under reduced protein density surfaces will enable circumventing MTL, typically observed for high affinity small molecule interactions with the K_D value less than 100nM. Although further optimization of assay conditions might be required, we do not anticipate any significant challenge to integrate and streamline the use of MASS-1 for FBDD, especially during the characterization of optimized lead molecule.

Apart from being a high-throughput SPRi biosensor, sensitivity of MASS-1 allowed the characterization of picomolar affinity interaction by overcoming MTL (Figure 8). Exclusion of the k_m factor in the fitting model failed to fit the binding data generated for the highest density mAb surfaces used in this study (**Supplementary Figure 2**) and yielded inaccurate rate constants. No significant difference in k_a, k_d, and K_D values was observed among the three surface densities tested following the inclusion of k_m factor in the fitting model (Table 3), suggesting that the model successfully compensated for observed MTL and extrapolated true kinetic values for all the three mAb-antigen interactions.

It is important to understand that mAb capture densities of 100RU, 260RU, and 320RU are routinely captured to determine their kinetic of binding to 97kD, 14kD or 3.5kD antigens, respectively (28). In this study, these densities are classified as high based on the mAb density requirement for the kinetic analysis of the mAb-antigen interactions devoid of any MTL. Although inclusion of k_m in the fitting generated reliable kinetic values in this study, it is not always successful. We routinely observe that the model fails to compensate for observed MTL and generates inaccurate kinetic values (data not shown). Therefore, performing kinetic assays at surface densities that exhibit minimal to no MTL is preferred to measure reliable binding rate constants. The goal of this work was to demonstrate ability of MASS-1 sensitivity to design kinetic assays devoid of MTL using ultra-low density mAb surface required for the reliable measurement of binding rate constants of mAb-antigen interactions with k_a value greater than 10^6 $M^{-1}s^{-1}$. Although characterization of mAb-antigen interactions with slow dissociation rate would be a good addition to the current embodiment, it was beyond the scope of this study and would need further investigation.

Collectively, the extensive binding studies presented in this work demonstrate that MASS-1 is a reliable and sensitive SPRi biosensor with throughput comparable to the Biacore 4000. With an eight-channel parallel flow system, MASS-1 can reduce assay development time by permitting simultaneous study of various assay conditions across different flow channels. Moreover, MASS-1 provides an opportunity to simultaneously perform up to eight unique experiments across the different flow channels. The sensitivity of MASS-1 allows design of kinetic assays using ultra-low density ligand surfaces, and binding data generated with R_{max} of less than 4RU is highly reproducible, which is typically challenging to achieve using other SPR/SPRi biosensors.

We believe that the throughput and sensitivity of the MASS-1 biosensor will complement the Biacore 4000 and Biacore T200 biosensors of our HTS biomolecular group.

Although the primary rationale of this work was to evaluate the throughput and sensitivity of MASS-1, we also intended to shed some light on different experimental design aspects that should be considered while performing kinetic analysis on RT-LF platform. The various assay optimization considerations presented in this study are envisioned to be used as guidelines for the design of kinetic assays. Although a wide range of antigen molecular weights were selected based on the typical requirement of the biosensor user base, we did not include analyte molecular weights greater than 105kD, which could be considered as a limitation of our work. We understand that characterizing an extensive panel of mAb-antigen interactions is not necessary to evaluate performance of new biosensor. However, such data provide statistical significance on the correlation of the measured rate constants and in turn will give us higher confidence in the reliability of the binding kinetic parameters measured using the new biosensor. We believe that this work will provide a benchmark for future evaluations of new biosensor platforms.

ACKNOWLEDGEMENTS

We are thankful to Joel Martin and his group, especially Lisa Hersh's molecular cloning group and Raymond Leidich's team for purifying all of the recombinant proteins used in the study. We are grateful to Anke Watty and her group for developing stable CHO cell lines expressing the proteins used in this work. We are also thankful to Tammy Huang, David Buckler, Celestine Thomas, William Olson and Nicholas Papadopoulos for reviewing the manuscript and providing their valuable input. We sincerely appreciate JoAnne Bruno and Christopher Whalen from Sierra Sensors for providing technical input on designing SICK assay and also providing the MASS-1 schematic.

REFERENCES

1. Aggarwal, R. S. (2014) What's fueling the biotech engine-2012 to 2013. *Nat Biotechnol* **32**, 32-39
2. Elvin, J. G., Couston, R. G., and van der Walle, C. F. (2013) Therapeutic antibodies: market considerations, disease targets and bioprocessing. *Int J Pharm* **440**, 83-98
3. Walsh, G. (2014) Biopharmaceutical benchmarks 2014. *Nat Biotechnol* **32**, 992-1000
4. Nieri, P., Donadio, E., Rossi, S., Adinolfi, B., and Podesta, A. (2009) Antibodies for therapeutic uses and the evolution of biotechniques. *Curr Med Chem* **16**, 753-779
5. Andersson, K., Karlsson, R., Löfås, S., Franklin, G., and Hämäläinen, M. D. (2006) Label-free kinetic binding data as a decisive element in drug discovery. *Expert opinion on drug discovery* **1**, 439-446
6. Swinney, D. (2008) Applications of Binding Kinetics to Drug Discovery. *Pharm Med* **22**, 23-34
7. Swinney, D. C. (2009) The role of binding kinetics in therapeutically useful drug action. *Curr Opin Drug Discov Devel* **12**, 31-39
8. Navratilova, I., and Hopkins, A. L. (2011) Emerging role of surface plasmon resonance in fragment-based drug discovery. *Future medicinal chemistry* **3**, 1809-1820
9. Cooper, M. A. (2002) Optical biosensors in drug discovery. *Nature reviews. Drug discovery* **1**, 515-528
10. Wartchow, C. A., Podlaski, F., Li, S., Rowan, K., Zhang, X., Mark, D., and Huang, K. S. (2011) Biosensor-based small molecule fragment screening with biolayer interferometry. *Journal of computer-aided molecular design* **25**, 669-676
11. Canziani, G. A., Klakamp, S., and Myszka, D. G. (2004) Kinetic screening of antibodies from crude hybridoma samples using Biacore. *Analytical biochemistry* **325**, 301-307
12. Leonard, P., Safsten, P., Hearty, S., McDonnell, B., Finlay, W., and O'Kennedy, R. (2007) High throughput ranking of recombinant avian scFv antibody fragments from crude lysates using the Biacore A100. *J Immunol Methods* **323**, 172-179
13. Safsten, P., Klakamp, S. L., Drake, A. W., Karlsson, R., and Myszka, D. G. (2006) Screening antibody-antigen interactions in parallel using Biacore A100. *Anal Biochem* **353**, 181-190
14. VanWiggeren, G. D., Bynum, M. A., Ertel, J. P., Jefferson, S., Robotti, K. M., Thrush, E. P., Baney, D. M., and Killeen, K. P. (2007) A novel optical method providing for high-sensitivity and high-throughput biomolecular interaction analysis. *Sensors and Actuators B: Chemical* **127**, 341-349
15. Abdiche, Y. N., Lindquist, K. C., Pinkerton, A., Pons, J., and Rajpal, A. (2011) Expanding the ProteOn XPR36 biosensor into a 36-ligand array expedites protein interaction analysis. *Anal Biochem* **411**, 139-151
16. Drake, A. W., Tang, M. L., Papalia, G. A., Landes, G., Haak-Frendscho, M., and Klakamp, S. L. (2012) Biacore surface matrix effects on the binding kinetics and affinity of an antigen/antibody complex. *Anal Biochem* **429**, 58-69
17. Smith, E. A., and Corn, R. M. (2003) Surface Plasmon Resonance Imaging as a Tool to Monitor Biomolecular Interactions in an Array Based Format. *Applied spectroscopy* **57**, 320A-332A

18. Rich, R. L., and Myszka, D. G. (2011) The Revolution of Real-Time, Label-Free Biosensor Applications. in *Label-Free Technologies for Drug Discovery*, John Wiley & Sons, Ltd. pp 1-25
19. Navratilova, I., Eisenstien, E., and Myszka, D. G. (2005) Measuring long association phases using Biacore. *Anal Biochem* **344**, 295-297
20. Goldstein, B., Coombs, D., He, X., Pineda, A. R., and Wofsy, C. (1999) The influence of transport on the kinetics of binding to surface receptors: application to cells and BIAcore. *J Mol Recognit* **12**, 293-299
21. Myszka, D. G., He, X., Dembo, M., Morton, T. A., and Goldstein, B. (1998) Extending the range of rate constants available from BIACORE: interpreting mass transport-influenced binding data. *Biophys J* **75**, 583-594
22. Schuck, P., and Zhao, H. (2010) The role of mass transport limitation and surface heterogeneity in the biophysical characterization of macromolecular binding processes by SPR biosensing. *Methods Mol Biol* **627**, 15-54
23. Glaser, R. W. (1993) Antigen-Antibody Binding and Mass Transport by Convection and Diffusion to a Surface: A Two-Dimensional Computer Model of Binding and Dissociation Kinetics. *Analytical biochemistry* **213**, 152-161
24. Karlsson, R., Roos, H., Fägerstam, L., and Persson, B. (1994) Kinetic and Concentration Analysis Using BIA Technology. *Methods* **6**, 99-110
25. Katsamba, P. S., Navratilova, I., Calderon-Cacia, M., Fan, L., Thornton, K., Zhu, M., Bos, T. V., Forte, C., Friend, D., Laird-Offringa, I., Tavares, G., Whatley, J., Shi, E., Widom, A., Lindquist, K. C., Klakamp, S., Drake, A., Bohmann, D., Roell, M., Rose, L., Dorocke, J., Roth, B., Luginbühl, B., and Myszka, D. G. (2006) Kinetic analysis of a high-affinity antibody/antigen interaction performed by multiple Biacore users. *Anal Biochem* **352**, 208-221
26. Rich, R. L., Papalia, G. A., Flynn, P. J., Furneisen, J., Quinn, J., Klein, J. S., Katsamba, P. S., Waddell, M. B., Scott, M., Thompson, J., Berlier, J., Corry, S., Baltzinger, M., Zeder-Lutz, G., Schoenemann, A., Clabbers, A., Wieckowski, S., Murphy, M. M., Page, P., Ryan, T. E., Duffner, J., Ganguly, T., Corbin, J., Gautam, S., Anderluh, G., Bavdek, A., Reichmann, D., Yadav, S. P., Hommema, E., Pol, E., Drake, A., Klakamp, S., Chapman, T., Kernaghan, D., Miller, K., Schuman, J., Lindquist, K., Herlihy, K., Murphy, M. B., Bohnsack, R., Andrien, B., Brandani, P., Terwey, D., Millican, R., Darling, R. J., Wang, L., Carter, Q., Dotzlaf, J., Lopez-Sagaseta, J., Campbell, I., Torreri, P., Hoos, S., England, P., Liu, Y., Abdiche, Y., Malashock, D., Pinkerton, A., Wong, M., Lafer, E., Hinck, C., Thompson, K., Primo, C. D., Joyce, A., Brooks, J., Torta, F., Bagge Hagel, A. B., Krarup, J., Pass, J., Ferreira, M., Shikov, S., Mikolajczyk, M., Abe, Y., Barbato, G., Giannetti, A. M., Krishnamoorthy, G., Beusink, B., Satpaev, D., Tsang, T., Fang, E., Partridge, J., Brohawn, S., Horn, J., Pritsch, O., Obal, G., Nilapwar, S., Busby, B., Gutierrez-Sanchez, G., Gupta, R. D., Canepa, S., Witte, K., Nikolovska-Coleska, Z., Cho, Y. H., D'Agata, R., Schlick, K., Calvert, R., Munoz, E. M., Hernaiz, M. J., Bravman, T., Dines, M., Yang, M.-H., Puskas, A., Boni, E., Li, J., Wear, M., Grinberg, A., Baardsnes, J., Dolezal, O., Gainey, M., Anderson, H., Peng, J., Lewis, M., Spies, P., Trinh, Q., Bibikov, S., Raymond, J., Yousef, M., Chandrasekaran, V., Feng, Y., Emerick, A., Mundodo, S., Guimaraes, R., McGirr, K., Li, Y.-J., Hughes, H., Mantz, H., Skrabana, R., Witmer, M., Ballard, J., Martin, L., Skladal, P., Korza, G., Laird-Offringa, I., Lee, C. S., Khadir, A., Podlaski, F., Neuner, P., Rothacker, J., Rafique, A., Dankbar, N., Kainz,

P., Gedig, E., Vuyisich, M., Boozer, C., Ly, N., Toews, M., Uren, A., Kalyuzhniy, O., Lewis, K., Chomey, E., Pak, B. J., and Myszka, D. G. (2009) A global benchmark study using affinity-based biosensors. *Analytical biochemistry* **386**, 194-216

27. Cannon, M. J., Papalia, G. A., Navratilova, I., Fisher, R. J., Roberts, L. R., Worthy, K. M., Stephen, A. G., Marchesini, G. R., Collins, E. J., Casper, D., Qiu, H., Satpaev, D., Liparoto, S. F., Rice, D. A., Gorshkova, I. I., Darling, R. J., Bennett, D. B., Sekar, M., Hommema, E., Liang, A. M., Day, E. S., Inman, J., Karlicek, S. M., Ullrich, S. J., Hodges, D., Chu, T., Sullivan, E., Simpson, J., Rafique, A., Luginbühl, B., Westin, S. N., Bynum, M., Cachia, P., Li, Y.-J., Kao, D., Neurauter, A., Wong, M., Swanson, M., and Myszka, D. G. (2004) Comparative analyses of a small molecule/enzyme interaction by multiple users of Biacore technology. *Analytical biochemistry* **330**, 98-113

28. Myszka, D. G., Morton, T. A., Doyle, M. L., and Chaiken, I. M. (1997) Kinetic analysis of a protein antigen-antibody interaction limited by mass transport on an optical biosensor. *Biophys Chem* **64**, 127-137

Title: Exploring Sensitivity & Throughput of a Parallel Flow SPRi Biosensor for Characterization of Antibody-Antigen Interaction

Figure Legends

Figure 1 MASS-1 can simultaneously inject up to eight different samples into independent flow cells, labeled as Channel-1 through Channel-8. Each flow channel contains two individually addressable detection spots (designated as Spot-A and Spot-B), for a total of 16 binding measurements across the entire sensor surface.

Figure 2 Comparable density of mAb was first captured across different flow channels (Channel-1 through Channel-8) on HCA sensors immobilized with anti-human Fcγ capture mAb. Different concentrations of antigen (serially diluted two-fold) were injected over the mAb capture surface for 4 minutes and dissociation of bound antigen in running buffer was observed for 10 minutes. Real time binding sensorgrams of mAb binding to 20kD **(A)**, 28kD **(B)**, 48kD **(C)**, 77kD **(D)**, and 92kD **(E)** antigen are shown as black lines while red lines represent model fits generated by globally fitting real-time binding data using a 1:1 binding model with mass transport limitation. Binding sensorgrams comprise at least duplicate injections of same antigen concentration. All mAb-antigen binding interactions were also characterized on Biacore 4000 platform under comparable experimental conditions and the binding sensorgrams along with the global fits are presented. Highest antigen concentration used to fit binding data is provided and binding kinetics values generated are provided in Table 1.

Figure 3 Correlation factor was determined by calculating the ratio of kinetics values measured on Biacore 4000 to those determined on MASS-1 for mAbs captured across different flow channels. Correlation factor calculated for k_a **(A)**, k_d **(B)** and K_D **(C)** measured across different flow channels of MASS-1 for mAb binding to 20kD (●), 28kD (●), 48kD (●), 77kD (●), and 92kD (●) antigen are plotted. Serrated red lines indicate a three-fold difference in the kinetic values with a correlation factor of 3 and 0.33.

Figure 4 The same mAb is first captured across flow channels 1 through 8 **(A)** followed by the injection of eight concentration series of analyte over mAb captured surfaces **(B)**. Binding rate constants are measured by running two cycles – buffer injection cycle (for second reference subtraction) followed by the injection of eight concentration titers of analyte.

Figure 5 mAb binding to 14kD **(A)**, 18kD **(B)**, 28kD **(C)**, 29kD **(D)**, 38kD **(E)**, 48kD **(F)**, 77kD **(G)**, and 105kD **(H)** antigen was first captured either following SICK assay format on MASS-1 or using the standard MICK assay format on both MASS-1 and Biacore 4000. Two mAbs per antigen were included in this study referred as mAb# 1 & mAb# 2. Different concentrations of antigen serially diluted by two-fold were injected for 4 minutes followed by 10 minutes of dissociation. Overlay of at least triplicate injections of the same antigen concentration is shown in black lines while red lines represent global fits of real-time binding data. The highest concentration used to fit data is shown and kinetics values measured using SICK and MICK assay formats are provided in Table 2. To ensure that our analysis did not introduce any unintended biasing in the measurement of rate constants, all of the binding data generated using the SICK or MICK assay formats on Biacore 4000 and MASS-1 were independently analyzed by adopting the "blind analysis" technique. During the analysis, the antigen concentrations that yielded the best global fits of the double reference subtracted data were selected. This resulted in the incorporation of different antigen concentrations for few interactions as shown in the figure. However, this discrepancy in antigen concentrations used to fit the data did not influence the values of measured kinetics parameters (Table 2).

Figure 6 Scatterplot showing correlation between k_a **(A)**, k_d **(B)** and K_D **(C)** values measured using SICK and MICK assay formats on MASS-1 platform for mAbs binding to 14kD (●), 18kD (●), 28kD (●), 29kD (●), 38kD (●), 48kD (●), 77kD (●), and 105kD (●) antigen is shown. Also plotted is correlation between k_a **(D)**, k_d **(E)** and K_D **(F)** values measured using SICK assay on MASS-1 biosensor and MICK assay performed on Biacore 4000. Serrated black line signifies correlation coefficient of 1 while serrated red lines indicate three-fold difference in kinetic values for mAbs binding to different molecular weight antigens.

Figure 7 The HCA sensor was first immobilized with different densities of anti-human Fcγ capture mAb (approximately 400RU, 1000RU, 2500RU & 10000RU) using standard EDC-NHS surface chemistry detailed in the Materials and Methods section. A comparable low density of mAb binding to 14kD **(A)**, 18kD **(B)**, 28kD **(C)**, 29kD **(D)**, and 39kD **(E)** antigen was first captured on anti-human Fcγ, immobilized at different surface densities. Varying concentrations of specific antigen (serially diluted by two-fold in running buffer) were injected over mAb captured surface for 4 minutes followed by 10 minutes of dissociation step. Real-time binding of triplicate injections of similar antigen concentration binding to captured mAb is shown in black while global fits generated to calculate kinetics values are shown in red. The highest antigen concentration used to fit binding data is provided and binding kinetics parameters are tabulated in Table 3.

Figure 8 Different levels of mAb to 97kD **(A, D)**, 14kD **(B, E)**, and 3.5kD **(C, F)** antigen were first captured using anti-human Fcγ as indicated. Varying concentrations of antigen (two-fold serial dilution in running buffer) were injected over different mAb surfaces for 6 minutes followed by 15 minutes dissociation. The overlay of triplicate injections of each antigen concentration is shown as black lines and global fitting of real time binding data using 1:1 binding model with mass transport limitation is shown in red. The highest antigen concentration used to fit binding data is also shown and the calculated binding kinetics values are tabulated in **Error! Reference source not found.**. Binding response observed for 97kD **(D)**, 14kD **(E)**, and 3.5kD **(F)** antigen at indicated concentration was normalized based on the maximum binding signal (R_{max}) observed for respective mAb surface densities to demonstrate MTL. Since the binding curve for 14kD antigen was significantly dominated by MTL when the 260RU surface was used for measurement, we experienced difficulty in fitting the binding data even after incorporating k_m in the fitting model (data not shown). The default initial k_m value of 10^{10} used by the Scrubber fitting software yielded erroneous kinetic values and hence the initial k_m value had to be empirically changed to generate the fits shown in **B.**

Figure 9 Depending on the molecular weight of the antigen, different levels of mAb binding to 14kD (A), 21kD (B), 29kD (C), 48kD (D), 77kD (E), and 97kD (F) antigen was captured using anti-human Fcγ followed by injection of different concentrations of antigen serially diluted by three-fold. To avoid non-specific binding of 30kD antigen, kinetic studies were performed in HBS-ET running buffer supplemented with 450mM sodium chloride (final concentration). Real time binding sensorgrams of duplicate injection for same antigen concentration is shown in black. The highest antigen concentration used to fit binding data is provided. Global fits obtained using 1:1 binding model with mass transport limitation is represented by red lines and calculated binding kinetics parameters are tabulated in Table V. "Blind analysis" technique of double reference subtracted binding sensorgrams was performed (as described in Figure 5) and the concentration series used to fit the binding curve generated using MASS-1 and Biacore 4000 were found to be different for few mAb-antigen interactions (mAb-3, mAb-10, mAb-12, mAb-13). However, no significant difference in their respective measured kinetics values was observed.

Figure 10 Graphical representation revealing correlation of binding kinetics values measured for 189 mAbs binding to antigens with molecular weights of 14kD (●), 21kD (●), 28kD (●), 29kD (●), 30kD (●), 32kD (●), 38kD (●), 48kD (▼), 68kD (▼), 77kD (▼), 92kD (▼), 97kD (▼), and 105kD (▼) is shown. Scatterplot of average values of k_a **(A)**, k_d **(B)** and K_D **(C)** measured from three independent experiments using Biacore 4000 and MASS-1 is shown. Correlation factor of 1 is shown as serrated black line while three-fold difference in the kinetic values is shown as serrated red line.

Supplementary Figure 1 Image of HCA sensor surface representing flow channels with different immobilization levels of anti-hFcγ capture molecule

Supplementary Figure 2 Different levels of mAb binding to 97kD **(A)**, 14kD **(B)**, or 3.5kD **(C)** antigen was first captured using anti-hFcγ as indicated. Varying concentrations of antigen (2-fold serial dilution) were injected over different mAb surfaces for 6 minutes followed by 15 minutes dissociation. Real time antigen binding is color coded based on antigen concentrations and fits generated by globally fitting the binding data using 1:1 binding model without mass transport limitation is shown in black serrated lines. Residual plots showing difference between experimental data and fits generated is also shown. Poor fits of binding data generated at higher density mAb surfaces is reflected by non-random distribution of residual plot with residual signal >5% of binding response. Residual plot for lowest density mAb surface is randomly distributed around 0 RU.

	mAb Captured	Kinetic Parameters	Channel 1	Channel 2	Channel 3	Channel 4	Channel 5	Channel 6	Channel 7	Channel 8	Average ± Std Dev	Biacore
20kD Antigen	mAb-1	k_a (1/Ms)	4.74E+04	4.84E+04	4.67E+04	4.80E+04	4.74E+04	4.68E+04	4.66E+04	4.83E+04	(4.74 ± 0.07) E+04	4.64E+04
		k_d (1/s)	1.02E-02	1.00E-02	9.97E-03	1.04E-02	1.05E-02	1.00E-02	1.07E-02	9.89E-03	(1.02 ± 0.03) E-03	1.35E-02
		K_D (M)	2.16E-07	2.07E-07	2.13E-07	2.17E-07	2.22E-07	2.14E-07	2.30E-07	2.05E-07	(2.15 ± 0.08) E-07	2.90E-07
	mAb-2	k_a (1/Ms)	7.25E+04	7.58E+04	7.68E+04	7.63E+04	7.24E+04	7.74E+04	6.29E+04	8.41E+04	(7.48 ± 0.60) E+04	7.19E+04
		k_d (1/s)	2.59E-03	2.59E-03	2.56E-03	2.54E-03	2.62E-03	2.53E-03	2.70E-03	2.56E-03	(2.58 ± 0.05) E-03	4.06E-03
		K_D (M)	3.57E-08	3.42E-08	3.33E-08	3.33E-08	3.61E-08	3.27E-08	4.28E-08	3.04E-08	(3.48 ± 0.37) E-08	5.65E-08
	mAb-3	k_a (1/Ms)	1.58E+05	1.76E+05	1.64E+05	1.62E+05	1.56E+05	1.68E+05	1.49E+05	1.64E+05	(1.62 ± 0.08) E+05	1.51E+05
		k_d (1/s)	5.86E-04	5.96E-04	5.93E-04	5.97E-04	5.79E-04	6.02E-04	6.04E-04	6.03E-04	(5.95 ± 0.09) E-04	8.77E-04
		K_D (M)	3.70E-09	3.38E-09	3.62E-09	3.69E-09	3.72E-09	3.58E-09	4.07E-09	3.68E-09	(3.68 ± 0.19) E-09	5.82E-09
28kD Antigen	mAb-4	k_a (1/Ms)	1.39E+06	1.39E+06	1.48E+06	1.44E+06	1.33E+06	1.51E+06	1.36E+06	1.38E+06	(1.41 ± 0.06) E+06	2.52E+06
		k_d (1/s)	3.52E-02	3.35E-02	3.51E-02	3.50E-02	3.54E-02	3.54E-02	3.44E-02	3.27E-02	(3.46 ± 0.10) E-02	7.43E-02
		K_D (M)	2.53E-08	2.40E-08	2.37E-08	2.44E-08	2.67E-08	2.34E-08	2.52E-08	2.37E-08	(2.46 ± 0.11) E-08	2.94E-08
	mAb-5	k_a (1/Ms)	6.65E+05	6.53E+05	6.51E+05	6.64E+05	6.72E+05	6.50E+05	6.68E+05	6.77E+05	(6.62 ± 0.10) E+05	9.94E+05
		k_d (1/s)	2.43E-03	2.46E-03	2.49E-03	2.52E-03	2.48E-03	2.56E-03	2.45E-03	2.45E-03	(2.48 ± 0.04) E-03	2.39E-03
		K_D (M)	3.66E-09	3.76E-09	3.82E-09	3.79E-09	3.69E-09	3.94E-09	3.67E-09	3.61E-09	(3.74 ± 0.11) E-09	2.41E-09
	mAb-6	k_a (1/Ms)	1.43E+05	1.61E+05	1.56E+05	1.52E+05	1.50E+05	1.54E+05	1.51E+05	1.53E+05	(1.52 ± 0.05) E+05	1.48E+05
		k_d (1/s)	6.93E-04	6.93E-04	6.99E-04	6.89E-04	7.22E-04	6.91E-04	7.08E-04	7.05E-04	(7.00 ± 0.11) E-04	7.83E-04
		K_D (M)	4.84E-09	4.31E-09	4.47E-09	4.54E-09	4.83E-09	4.48E-09	4.70E-09	4.61E-09	(4.60 ± 0.18) E-09	5.28E-09
48kD Antigen	mAb-7	k_a (1/Ms)	2.51E+05	2.50E+05	2.53E+05	2.54E+05	2.51E+05	2.39E+05	2.49E+05	2.46E+05	(2.49 ± 0.05) E+05	2.03E+05
		k_d (1/s)	8.87E-04	8.96E-04	8.83E-04	9.14E-04	8.82E-04	8.86E-04	9.09E-04	8.95E-04	(8.94 ± 0.12) E-04	1.04E-03
		K_D (M)	3.53E-09	3.58E-09	3.49E-09	3.60E-09	3.51E-09	3.71E-09	3.65E-09	3.64E-09	(3.59 ± 0.08) E-09	5.12E-09
	mAb-8	k_a (1/Ms)	3.19E+05	3.11E+05	3.11E+05	3.15E+05	3.08E+05	3.01E+05	3.16E+05	3.07E+05	(3.11 ± 0.06) E+05	2.57E+05
		k_d (1/s)	2.09E-04	2.16E-04	2.15E-04	2.20E-04	2.12E-04	2.11E-04	2.07E-04	2.23E-04	(2.14 ± 0.05) E-04	2.82E-04
		K_D (M)	6.56E-10	6.96E-10	6.92E-10	6.99E-10	6.88E-10	7.03E-10	6.54E-10	7.25E-10	(6.89 ± 0.24) E-10	1.10E-09
	mAb-9	k_a (1/Ms)	7.36E+05	7.08E+05	6.85E+05	7.06E+05	6.86E+05	6.80E+05	6.97E+05	6.98E+05	(6.99 ± 0.18) E+05	6.05E+05
		k_d (1/s)	1.21E-04	1.35E-04	1.24E-04	1.52E-04	1.41E-04	1.30E-04	1.40E-04	1.32E-04	(1.34 ± 0.10) E-04	2.12E-04
		K_D (M)	1.65E-10	1.90E-10	1.81E-10	2.15E-10	2.05E-10	1.92E-10	2.01E-10	1.90E-10	(1.92 ± 0.15) E-10	3.50E-10
	mAb-10	k_a (1/Ms)	5.74E+06	5.53E+06	5.83E+06	5.48E+06	5.58E+06	5.25E+06	5.29E+06	6.13E+06	(5.60 ± 0.29) E+06	4.63E+06
		k_d (1/s)	1.88E-04	1.66E-04	1.65E-04	1.83E-04	1.78E-04	1.84E-04	1.79E-04	1.85E-04	(1.78 ± 0.09) E-04	2.53E-04

77kD Antigen		K_D (M)	3.27E-11	2.99E-11	2.83E-11	3.34E-11	3.19E-11	3.50E-11	3.39E-11	3.02E-11	(3.19 ± 0.23) E-11	5.45E-11
	mAb-11	k_a (1/Ms)	1.10E+06	1.04E+06	1.06E+06	1.07E+06	1.03E+06	1.06E+06	1.03E+06	1.06E+06	(1.06 ± 0.02) E+6	6.68E+05
		k_d (1/s)	1.39E-04	1.46E-04	1.40E-04	1.33E-04	1.37E-04	1.40E-04	1.44E-04	1.43E-04	(1.40 ± 0.04) E-04	2.53E-04
		K_D (M)	1.26E-10	1.41E-10	1.32E-10	1.24E-10	1.33E-10	1.32E-10	1.39E-10	1.35E-10	(1.33 ± 0.06) E-10	3.79E-10
	mAb-12	k_a (1/Ms)	1.90E+06	1.86E+06	1.91E+06	1.90E+06	1.89E+06	1.87E+06	1.89E+06	1.80E+06	(1.88 ± 0.04) E+06	1.26E+06
		k_d (1/s)	1.60E-04	1.62E-04	1.65E-04	1.55E-04	1.53E-04	1.75E-04	1.54E-04	1.80E-04	(1.63 ± 0.10) E-04	2.46E-04
		K_D (M)	8.42E-11	8.73E-11	8.64E-11	8.14E-11	8.08E-11	9.32E-11	8.15E-11	1.00E-10	(8.69 ± 0.68) E-11	1.95E-10
92kD Antigen	mAb-13	k_a (1/Ms)	1.34E+05	1.36E+05	1.42E+05	1.45E+05	1.37E+05	1.28E+05	1.42E+05	1.22E+05	(1.36 ± 0.08) E+05	1.52E+05
		k_d (1/s)	1.33E-02	1.29E-02	1.35E-02	1.32E-02	1.36E-02	1.35E-02	1.32E-02	1.33E-02	(1.33 ± 0.02) E-02	1.60E-02
		K_D (M)	9.89E-08	9.49E-08	9.54E-08	9.09E-08	9.93E-08	1.06E-07	9.35E-08	1.09E-07	(9.85 ± 0.63) E-08	1.05E-07
	mAb-14	k_a (1/Ms)	6.76E+04	7.20E+04	6.95E+04	7.27E+04	6.79E+04	6.95E+04	6.94E+04	7.02E+04	(6.98 ± 0.18) E+04	7.19E+04
		k_d (1/s)	7.33E-04	7.10E-04	7.25E-04	7.10E-04	7.66E-04	7.34E-04	7.25E-04	7.32E-04	(7.29 ± 0.18) E-05	8.48E-04
		K_D (M)	1.08E-08	9.87E-09	1.04E-08	9.76E-09	1.13E-08	1.06E-08	1.05E-08	1.04E-08	(1.05 ± 0.05) E-08	1.18E-08
	mAb-15	k_a (1/Ms)	8.71E+04	9.21E+04	9.05E+04	9.34E+04	8.56E+04	8.67E+04	9.03E+04	8.60E+04	(8.90 ± 0.30) E+04	6.78E+04
		k_d (1/s)	1.57E-04	1.55E-04	1.54E-04	1.56E-04	1.69E-04	1.58E-04	1.60E-04	1.68E-04	(1.60 ± 0.06) E-04	1.22E-04
		K_D (M)	1.80E-09	1.68E-09	1.70E-09	1.66E-09	1.98E-09	1.82E-09	1.77E-09	1.95E-09	(1.80 ± 0.12) E-09	1.80E-09

		MICK Assay			SICK Assay			Biacore 4000 Assay		
Antigen Molecular Weight	mAb Captured	k_a (1/Ms)	k_d (1/s)	K_D (M)	k_a (1/Ms)	k_d (1/s)	K_D (M)	k_a (1/Ms)	k_d (1/s)	K_D (M)
14kD	mAb# 1	3.65E+05	1.52E-04	4.26E-10	2.80E+05	1.36E-04	4.87E-10	3.39E+05	1.96E-04	5.78E-10
	mAb# 2	3.85E+05	6.35E-04	1.66E-09	2.59E+05	5.95E-04	2.29E-09	2.48E+05	7.17E-04	2.89E-09
18kD	mAb# 1	1.05E+05	2.43E-03	2.31E-08	1.20E+05	2.61E-03	2.18E-08	1.32E+05	2.36E-03	1.78E-08
	mAb# 2	1.93E+05	1.02E-03	5.27E-09	2.19E+05	1.06E-03	4.85E-09	2.02E+05	1.12E-03	5.52E-09
28kD	mAb# 1	4.70E+05	7.88E-04	1.68E-09	5.11E+05	8.67E-04	1.71E-09	4.68E+05	8.50E-04	1.82E-09
	mAb# 2	8.63E+05	2.03E-03	2.36E-09	8.62E+05	2.16E-03	2.51E-09	7.19E+05	2.28E-03	3.17E-09
29kD	mAb# 1	1.32E+06	7.00E-04	5.31E-10	2.20E+06	8.50E-04	4.11E-10	9.35E+05	7.72E-04	8.26E-10
	mAb# 2	7.29E+05	1.84E-04	2.52E-10	7.54E+05	1.55E-04	2.16E-10	4.85E+05	1.95E-04	4.03E-10
38kD	mAb# 1	3.13E+05	9.15E-04	2.93E-09	3.43E+05	9.24E-04	2.69E-09	3.00E+05	9.96E-04	3.32E-09
	mAb# 2	2.98E+06	3.60E-03	1.31E-09	2.16E+06	3.21E-03	1.49E-09	1.22E+06	3.03E-03	2.48E-09
48kD	mAb# 1	3.46E+05	8.80E-04	2.54E-09	3.78E+05	8.95E-04	2.37E-09	2.76E+05	9.46E-04	3.43E-09
	mAb# 2	3.28E+05	1.75E-04	5.34E-10	3.05E+05	1.85E-04	6.07E-10	2.07E+05	2.13E-04	1.03E-09
77kD	mAb# 1	1.40E+06	4.70E-05	3.35E-11	2.07E+06	4.91E-05	2.51E-11	1.54E+06	9.45E-05	6.14E-11
	mAb# 2	2.98E+06	1.02E-04	3.43E-11	3.30E+06	9.01E-05	2.76E-11	3.30E+06	1.57E-04	4.75E-11
105kD	mAb# 1	2.65E+05	1.70E-03	6.44E-09	2.11E+05	1.64E-03	7.76E-09	3.40E+05	1.53E-03	4.50E-09

105KD	mAb# 2	3.74E+05	1.55E-03	4.15E-09		2.57E+05	1.56E-03	6.05E-09		3.75E+05	1.37E-03	3.66E-09

		anti-hFc Immobilization Level			
Antigen Molecular Weight	**Kinetics Parameters**	**400RU**	**1,000RU**	**2,500RU**	**10,000RU**
14kD	k_a (1/Ms)	1.48E+05	1.52E+05	2.12E+05	1.85E+05
	k_d (1/s)	4.14E-02	4.09E-02	4.44E-02	3.95E-02
	K_D (M)	2.80E-07	2.69E-07	2.10E-07	2.13E-07
18kD	k_a (1/Ms)	8.61E+04	7.35E+04	1.03E+05	1.01E+05
	k_d (1/s)	3.34E-03	3.25E-03	3.25E-03	3.11E-03
	K_D (M)	3.87E-08	4.42E-08	3.17E-08	3.08E-08
28kD	k_a (1/Ms)	4.11E+05	4.62E+05	5.32E+05	8.12E+05
	k_d (1/s)	2.80E-03	2.66E-03	2.70E-03	2.35E-03
	K_D (M)	6.81E-09	5.75E-09	5.08E-09	2.89E-09
29kD	k_a (1/Ms)	2.80E+04	2.75E+04	3.10E+04	4.29E+04
	k_d (1/s)	1.53E-02	1.52E-02	1.68E-02	1.62E-02
	K_D (M)	5.47E-07	5.52E-07	5.43E-07	3.76E-07
39kD	k_a (1/Ms)	1.07E+05	1.04E+05	1.53E+05	1.63E+05
	k_d (1/s)	1.35E-03	1.24E-03	9.15E-04	9.04E-04
	K_D (M)	1.26E-08	1.20E-08	5.97E-09	5.55E-09

		Kinetics Parameters			
Antigen Molecular Weight	**mAb Capture Level (RU)**	k_m	k_a (1/Ms)	k_d (1/s)	K_D (M)
97kD (Ectodomain)	**100**	**2.38E+08**	**5.29E+06**	**1.53E-04**	**2.89E-11**
	35	**4.86E+08**	**4.68E+06**	**1.18E-04**	**2.52E-11**
	13	**1.00E+10**	**5.30E+06**	**1.07E-04**	**2.02E-11**
	4	**1.00E+10**	**5.68E+06**	**1.28E-04**	**2.26E-11**
14kD (Ectodomain)	**260**	**7.46E+07**	**3.38E+06**	**3.09E-04**	**9.13E-11**
	100	**9.79E+07**	**3.77E+06**	**2.65E-04**	**7.03E-11**
	35	**1.00E+10**	**3.81E+06**	**2.28E-04**	**5.98E-11**
	12	**1.00E+10**	**5.30E+06**	**2.66E-04**	**5.00E-11**
3.5kD (Secreted)	**320**	**1.02E+07**	**1.59E+06**	**1.50E-03**	**9.43E-10**
	150	**1.49E+07**	**2.94E+06**	**1.85E-03**	**6.27E-10**
	70	**1.59E+08**	**1.80E+06**	**1.40E-03**	**7.73E-10**
	30	**1.00E+10**	**1.56E+06**	**1.50E-03**	**9.57E-10**

		Biacore 4000			MASS-1		
Antigen Molecular Weight	mAb Captured	k_a ($1x10^5$ 1/Ms)	k_d ($1x10^{-4}$ 1/s)	K_D ($1x10^{-9}$ M)	k_a ($1x10^5$ 1/Ms)	k_d ($1x10^{-4}$ 1/s)	K_D ($1x10^{-9}$ M)
14kD	mAb-1	10.21 ± 0.25	2.04 ± 0.16	0.20 ± 0.02	7.46 ± 0.92	1.79 ± 0.14	0.24 ± 0.05
	mAb-2	6.12 ± 0.10	0.55 ± 0.39	0.09 ± 0.06	4.17 ± 0.59	0.75 ± 0.12	0.19 ± 0.06
	mAb-3	2.87 ± 0.16	3.83 ± 0.12	1.33 ± 0.04	1.58 ± 0.12	3.41 ± 0.33	2.17 ± 0.29
	mAb-4	15.8 ± 0.50	6.31 ± 0.09	0.40 ± 0.01	10.99 ± 2.27	5.03 ± 0.17	0.47 ± 0.12
21kD	mAb-5	1.65 ± 0.41	25.81 ± 2.61	16.50 ± 5.15	2.71 ± 1.53	22.07 ± 3.86	10.62 ± 6.74
	mAb-6	0.78 ± 0.04	16.27 ± 1.34	20.90 ± 1.92	0.78 ± 0.07	14.00 ± 1.45	18.03 ± 1.46
	mAb-7	0.59 ± 0.09	9.45 ± 1.51	16.47 ± 4.77	0.94 ± 0.20	7.24 ± 2.27	7.61 ± 0.83
	mAb-8	3.30 ± 0.26	5.56 ± 0.85	1.71 ± 0.37	2.88 ± 0.61	4.67 ± 0.97	1.62 ± 0.04
29kD	mAb-9	17.29 ± 5.04	704.00 ± 218.53	40.53 ± 1.12	14.12 ± 1.52	438.40 ± 37.29	31.10 ± 1.51
	mAb-10	2.24 ± 0.42	7.99 ± 0.48	3.68 ± 0.94	2.30 ± 0.52	7.19 ± 0.05	3.25 ± 0.86
	mAb-11	3.42 ± 0.80	4.38 ± 0.35	1.36 ± 0.47	3.88 ± 0.43	2.81 ± 0.10	0.73 ± 0.11
	mAb-12	10.12 ± 2.47	3.49 ± 0.16	0.36 ± 0.12	9.71 ± 2.54	3.09 ± 0.18	0.33 ± 0.08
48kD	mAb-13	1.41 ± 0.17	2.03 ± 0.67	1.44 ± 0.40	1.52 ± 0.23	1.14 ± 0.03	0.76 ± 0.14
	mAb-14	1.79 ± 0.17	9.54 ± 0.69	5.36 ± 0.52	2.07 ± 0.02	7.51 ± 0.21	3.63 ± 0.08
	mAb-15	3.26 ± 0.21	1.98 ± 0.60	0.61 ± 0.21	3.25 ± 0.001	1.09 ± 0.05	0.34 ± 0.02
	mAb-16	5.78 ± 0.75	2.18 ± 0.49	0.38 ± 0.05	6.00 ± 0.12	1.52 ± 0.02	0.25 ± 0.001
77kD	mAb-17	5.07 ± 0.06	1.49 ± 0.08	0.29 ± 0.01	7.06 ± 0.82	0.93 ± 0.05	0.13 ± 0.01
	mAb-18	13.76 ± 0.14	1.04 ± 0.07	0.08 ± 0.001	17.22 ± 0.55	0.59 ± 0.06	0.03 ± 0.001
	mAb-19	16.13 ± 0.41	1.37 ± 0.10	0.08 ± 0.01	20.42 ± 0.91	0.83 ± 0.12	0.04 ± 0.01
	mAb-20	34.81 ± 3.99	2.49 ± 0.13	0.07 ± 0.01	56.19 ± 2.76	1.78 ± 0.05	0.03 ± 0.001
97kD	mAb-21	5.78 ± 0.59	41.66 ± 3.33	7.29 ± 1.28	8.97 ± 2.21	38.37 ± 7.23	4.36 ± 0.65
	mAb-22	4.91 ± 1.27	6.13 ± 0.31	1.31 ± 0.39	5.66 ± 0.36	5.06 ± 0.23	0.90 ± 0.10
	mAb-23	8.13 ± 0.32	1.45 ± 0.38	0.18 ± 0.05	9.78 ± 0.31	0.76 ± 0.07	0.08 ± 0.01
	mAb-24	7.17 ± 0.49	3.66 ± 0.19	0.51 ± 0.03	9.43 ± 0.38	2.74 ± 0.04	0.29 ± 0.02